Fermi National Accelerator Laboratory

FERMILAB-Pub-94/089-T

PARTON DENSITIES at HIGH ENERGY

ERIC LAENEN and EUGENE LEVIN*

Theoretical Physics Group, Fermi National Accelerator Laboratory,
P.O. Box 500, Batavia, IL 60510, USA

April 1994

to appear in *Annual Review of Nuclear and Particle Science*

*On leave from Theory Department, St. Petersburg Nuclear Physics Institute, 188350, Gatchina, St. Petersburg, Russia.

Operated by Universities Research Association Inc. under contract with the United States Department of Energy

Contents

1 What do we know about QCD? 3

1.1 What is QCD ? 4
1.2 Basics of QCD. 6
1.3 The map of QCD. 9
1.4 The low density (pQCD) region. 10
1.5 Nonperturbative QCD (npQCD) region. 11
1.6 High density QCD (hdQCD). 11
1.7 How to penetrate the high density QCD region. 12

2 New physical phenomena at small x_B: 13

2.1 Increase of the gluon (quark) density at $x_B \to 0$. 14
2.2 A new scale for the deeply inelastic process at $x_B \to 0$. 16
2.3 Saturation of the gluon density. 17

3 Two scales of hardness at high energy. 18

3.1 Two scales of hardness for deeply inelastic processes. 18
3.2 Transverse momentum factorization. 20
3.3 Small k_t behavior of the one-jet inclusive cross section and Landau - Pomeranchuk suppression. 21
3.4 Parton cascade in real time. 23

4 Shadowing corrections and nonlinear evolution equation. 24

4.1 Qualitative derivation of nonlinear (GLR) evolution equation . . 24
4.2 The scale of the shadowing corrections (SC). 25
4.3 New scale of transverse momentum (the critical line). 26
4.3.1 The main property of a solution of the GLR equation . . 26
4.3.2 Trajectories. 27
4.3.3 Semi-classical solution to the GLR equation. 27
4.4 The physical meanning of new scale for the typical transverse momentum in the parton cascade. 29
4.5 Correlations. 29

5 A look at the first small x_B HERA data. 32

5.1 25 nb^{-1} experimental data. 32
5.2 The value of SC from HERA data. 32
5.3 Saturation of the parton density or different physics for "soft" and "hard" processes? 33

6 Predictions. **34**
6.1 The structure of the typical inelastic event. 34
6.2 Total cross section in QCD. 35
6.3 The Mueller - Navelet processes ("hot spot" hunting). 37
6.4 Diffraction Dissociation (DD). 38
6.5 Large Rapidity Gap (LRG) processes. 39
6.6 Interaction with a nucleus. 41
6.6.1 Why is a nucleus a better target? 41
6.6.2 How do the new phenomena anticipated in high density QCD manifest themselves in interactions with a nucleus? 43
6.6.3 The factorization theorem in nuclear scattering. 45

7 Conclusions. **45**
7.1 Phase transition. 46
7.2 Where we stand. 47

1 What do we know about QCD?

In this review we will address the high energy or small x_B behavior of parton densities and hopefully demonstrate that this is a problem that is one of the principle and most difficult problems of QCD. It should be solved before QCD can truly be considered to be the only serious candidate for a theory of strong interactions at high energy.

In perturbative QCD only the periphery of this problem can be explored; its kernel is nonperturbative. That is to say, at $x_B \to 0$ we deal with a dense system of partons, either in the initial or in the final state, in the weak coupling limit in which the aggregate interaction between partons becomes strong due to the large density of partons even though the coupling constant α_s is small. The theoretical understanding of such a system of partons, which will be probed experimentally at the new generation of accelerators (HERA, LHC, RHIC), is relevant to issues as diverse as the small x behavior of deep-inelastic structure functions, the structure of a typical inelastic event produced at high energy hadron-hadron or ion-ion collisions, the understanding of nuclear shadowing and the problem of baryon number nonconservation in electroweak theory at high energies.

Fortunately, at the time of writing we have the first experimental results from HERA, so we can adjust theoretical imagination to data. However the key

problems are still in developing new theoretical methods to study the small x_B behavior of parton densities. Thus we will discuss mainly the theoretical problems encountered in opening up the frontier region of small x in perturbative QCD. We will also consider new ideas on how to approach the nonperturbative regime of the deep-inelastic structure functions.

This reviews focusses on the physical problems that we face in the region of small x_B and on the principal ideas about how to approach them in this new kinematical region, rather than on the theoretical scrutiny of these ideas. Some familiarity with the parton model will facilitate the reading of this review, although we tried to be as self-contained as possible. The preprint version of this review is somewhat more expansive than the published version: section 4.5 is expanded and 6.6 has been added. Our hope is to draw the attention of a large part of the physics community, and not only experts in high energy physics to this unique opportunity to create and study a new system of quark and gluons, the *quark – gluon liquid* as the source of a typical inelastic event at the new generation of accelerators.

1.1 What is QCD ?

To make clear the origin of both QCD and our belief that QCD is the true theory of strong interaction, let us review the main lessons we learned from experiments that taught us what this theory should be. In other words, using hindsight, we would like to infer the QCD lagrangian from data.

1. In 1964 Gell-Mann and Zweig suggested the quark model [1] in order to describe the spectrum of observed hadrons, which it still does very well. They introduced three very curious particles, **quarks** (u,d,s), having fractional electrical charge and baryonic quantum number (see e.g. Table 10.1 in [3]). With these they reduced the veritable zoo of hadrons to simple combinations of these quarks (and antiquarks), mesons consisting of quark-antiquark pairs, and baryons of three quarks. *The first lesson* for the future theory was that its building blocks should be these few quarks, and not the plethora of hadrons.

2. In the next several years the necessity to enlarge the number of quarks was realized. Indeed, there are hadrons that consist of identical quarks (e.g. the Δ^{++}-hyperon, which consists of three u quarks). Due to the Pauli- principle one cannot build such baryons from quarks with a symmetrical coordinate wavefunction. However, it is impossible to have an antisymmetrical wavefunction for the lightest hadrons or in other words, for the multiquark state with the minimum energy. The only resolution to this puzzle was to increase the number of quarks by introducing a new quantum number, **color**[2]. One needs three colors for each quark flavor to describe the spectrum of baryons. E.g.

the Δ^{++}-hyperon consists of three differently colored u-quarks. So *the second lesson* from the spectrum of hadrons was that quarks are colored.

3. Attempts to find free quarks failed. Thus, one needed to build a theory that provides forces sufficiently strong at large distances to prevent quarks from existing outside of hadrons. For a relativistic theory we know that the only way to incorporate such a force is to assume that there is a **particle with zero mass** which mediates this force. Thus *the third lesson* was that there must a new particle. It was called *gluon*.

4. Unlike the photon in QED, the gluon could not be neutral with respect to the new color quantum number. In the QED-like case the potential energy in the Born approximation is equal to

$$V_{ij\to i'j'} = \frac{e_{ci}e_{cj}}{R}\delta(ii')\delta(jj') , \qquad (1)$$

where $i, j(i', j')$ are the colors of initial (final) quarks and R is the distance between quarks. Since the color of the antiquark has a sign opposite to that of the quark, it is easy to understand that the average V for mesons must be negative ($\langle M|V|M\rangle < 0$), while for a baryon the average V is still positive ($\langle B|V|B\rangle > 0$). Thus a theory with a neutral gluon had no chance to describe the spectrum of hadrons. The only way to construct a theory of quarks (antiquarks) and gluons is to assume that **gluons** also **carry color**. As far as their color properties are concerned, we can imagine each gluon as a quark-antiquark pair. In this case we can rewrite eq.(1) in the form

$$V_{ij\to i'j'} = [\frac{1}{N_c}\delta(ii')\delta(jj') + \frac{1}{2}\delta(ij')\delta(ji')]\frac{1}{R} . \qquad (2)$$

Eq.(2) provides negative V for both mesons and baryons ($\langle M|V|M\rangle < 0$; $\langle B|V|B\rangle < 0$). So *the fourth lesson* was that gluons are also colored.

5. Now we are almost ready to write down the lagrangian of our theory. The only additional idea that we should incorporate is gauge invariance. It ensures the masslessness of the gluon to all orders in perturbation theory, which is necessary for confinement. Thus we arrive at *the fifth lesson*, namely that the theory should be gauge invariant.

Already in 1954 Yang and Mills wrote down the lagrangian of a theory with all the above properties [4]. Using their result Fritzsch, Gell-Mann and Leutwyler [5] suggested the following lagrangian[1]:

$$L = \sum_f \bar{\psi}_f [iD(A) - m_f]\psi_f - \tfrac{1}{4}F^2(A) , \qquad (3)$$

[1]The full quantum lagrangian of can be found e.g. in the Handbook of Perturbative QCD written by the CTEQ Collaboration [6], the part that is written here, the classical action, suffices to understand small x interactions.

where the index f runs of the quark flavors $(u,d,s,..)$, and the covariant derivative D and the gluon field strength F are defined in terms of the gluon vector field A_b^μ as follows:

$$D_{\mu,ij}(A) = \partial_\mu \delta_{ij} + igA_{\mu a}(T_a)_{ij}\,; \tag{4}$$

$$F_{\mu\nu,a} = \partial_\mu A_{\nu a} - \partial_\nu A_{\mu a} - gC_{abc}A_{\mu b}A_{\nu c}\,. \tag{5}$$

Indices μ and ν refer to spacetime coordinates and i,j and a,b,c refer to the color of quarks and gluons (for details see ref.[6]).

The lagrangian of eq.(3) generates the interaction between quarks and gluons as well as the gluon self-interaction, see Fig.1. The former looks very similar to the interaction in QED while the latter is the manifestation of the fact that gluon carries the color quantum number. It is a distinctive feature of QCD, and is especially important for the small x_B behavior of parton densities, as will become clear further on.

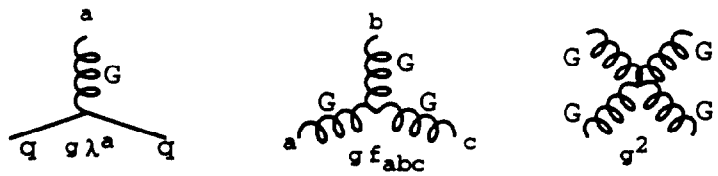

Figure 1: The interaction between quarks (q) and gluons (G) generated by the QCD Lagrangian of eq.(3).

1.2 Basics of QCD.

Having hopefully convinced the reader in the first subsection that QCD is the theory one obtains by examining experimental data, we will now discuss the feedback, i.e. the predictions of QCD that have been checked experimentally.

1. Asymptotic freedom.

The first and the greatest prediction was asymptotic freedom. This is the fact that the coupling constant of QCD $\alpha_s(1/r^2)$ becomes small at short distances [7] (the exact opposite behavior occurs in QED, as first shown by Landau [8])

$$\alpha_s(\frac{1}{r^2}) = \frac{4\pi}{b\ln\frac{1}{r^2\Lambda}} = \frac{\alpha_s(\mu^2)}{1 + \alpha_s(\mu^2)\frac{b}{4\pi}\ln\frac{1}{r^2\mu^2}}\,, \tag{6}$$

where $b = 11 - \frac{2}{3}n_f$ and n_f is the number of quarks (here the number of colors (N_c) is equal 3). The scale μ is the renormalization scale.

To understand the importance of this result it is enough to mention that the whole of perturbation theory is based on this remarkable property, and on the

existence of a factorization theorem, to be discussed momentarily. Asymptotic freedom has been checked experimentally, as is shown convincingly in Fig.2.

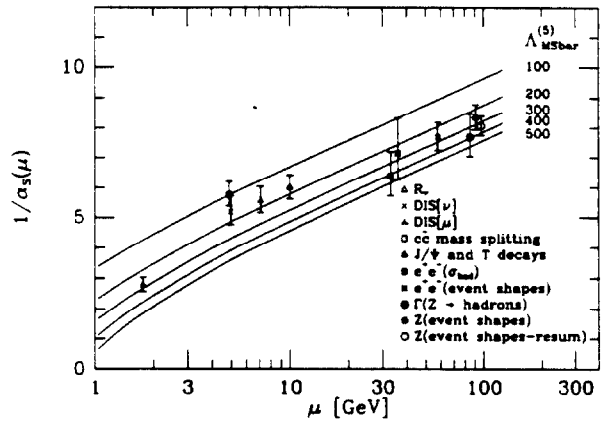

Figure 2: The running of the QCD coupling constant. The various symbols correspond to different experiments used to measure α_S.

2. QCD bremsstrahlung.

A striking result from e^+e^- colliders during the last two decades (especially from LEP) is that the QCD bremsstrahlung of massless gluons describes quite well the hadron distribution in a jet (see ref.[13] e.g.). The study of isolated jets however is no longer a prerogative of e^+e^- collision experiments but has become standard staple also for hadron colliders (see ref.[14]). Let us list some of the main properties of QCD for jet decay, which have been confirmed experimentally.

1. Produced hadrons exist in several clearly separated angular clusters, which are moreover well mimicked by distributions of massless gluons typical for bremsstrahlung processes.

2. Ratios of cross sections for different numbers of jets in the final state coincide with the corresponding pQCD calculation, assuming that each jet is the result of decay of a produced parton (quark or gluon). Both the ALEPH and DELPHI collaborations at LEP have measured the ratio of four- to three jet production ($\frac{\sigma(e^+e^-\to 4jets)}{\sigma(e^+e^-\to 3jets}$), which effectively measures the value of the triple gluon vertex (see Fig.1), and found that its value agrees with the QCD prediction [15]. This experimental fact then is a direct observation that gluons carry the color charge.

3. The hump-backed form of the inclusive cross section in e^+e^- annihilation, indicative of coherence effects in jet decays and predicted in QCD (see ref.[16])

has been established quite well by now. Other manifestations of coherence have been predicted and measured [13][14].

3. Factorization.

The factorization theorem [17] is the basis of all applications of perturbative QCD to so-called hard processes with hadrons in the initial state. To be able to apply it one needs the presence of a large scale in the process. Let us, following the CTEQ handbook [6], illustrate this theorem using the simple example of high p_t (the large scale) single hadron inclusive production in hadron - hadron collisions $A(p_A) + B(p_B) \rightarrow C(p_C) + X$. The factorization theorem reads

$$E_C \frac{d\sigma}{d^3p_C} = \sum_{abc} \int dx_a dx_b \frac{dz}{z} \phi_{a/A}(x_a,\mu)\phi_{b/B}(x_b,\mu)|\vec{k}_c| \frac{d\hat{\sigma}}{d^3k_c}(\frac{p_c}{z\sqrt{s}},\mu) D_{C/c}(z,\mu) \tag{7}$$

where all notation is clear from Fig.3. Here μ is the factorization scale, which, although arbitrary, is in practical cases best chosen near the relevant large scale of the process in order to avoid the occurrence of large logarithms in the perturbative expansion for $d\hat{\sigma}/d^3k_c$.

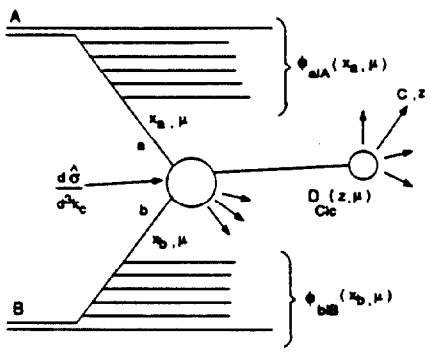

Figure 3. The factorization theorem, eq.(7), for single particle inclusive hadron production at large p_t.

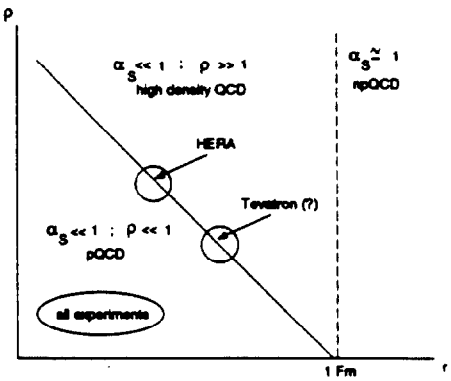

Figure 4. The map of QCD. ρ is the density of partons (gluons) in the transverse plane (see eq.(6)) and r is the distance resolved by an experiment.

The physical meaning of the factorization theorem is easily understood (unlike the proof [17]): it factorizes the scattering process into three stages:

1. The probability of the reaction is equal to the product of the probabilities to find partons a and b inside the hadrons A and B, i.e. the product of the two parton densities[2] $\phi_{a/A}$ and $\phi_{b/B}$ in eq.(7). These parton densities should be

[2]The parton densities $\phi_{a/A}$ are also commonly referred to as parton distribution functions.

measured in another reaction at a certain scale. For other values of μ they can then be determined via the GLAP evolution equation, to be discussed later.

2. A hard production process involving the parton with large transverse momentum (k_{tc} in eq.(7)). This process occurs at a short distance R, where $\frac{1}{\mu} \ll R \ll \frac{1}{k_{tc}}$ and can be systematically calculated order by order in perturbation theory.

3. In the final state the probability to find hadron C is given by the fragmentation function that describes the decay of parton c to many hadrons among which is hadron C.

The factorization formula has been checked experimentally; the most impressive result came from CDF (see review [14] e.g., and [27]) where the one jet inclusive cross section with large transverse momentum was measured. The factorization theorem was able to describe the experimental data in a kinematical region where the value of cross section falls over seven orders of magnitude within an accuracy of 10 -20 %.

1.3 The map of QCD.

Having described the basic features of QCD, we will start to answer in this subsection the following questions: (i) What we have learned about QCD; (ii) What problems are still unsolved in QCD?; (iii) Can we relate the kinematical region in which we have to face these unsolved problems to collision processes?

Fig.4 displays the 'map of QCD'. Shown are three separate regions, distinguished by the size of the variables Q^2 and x, which will be defined momentarily. Each region corresponds to quite different physics and enjoys a different level of understanding. Before we discuss these three regions in more detail let us introduce the necessary notational conventions and definitions.

In Fig.4 r is the distance that can be resolved by the scattering process under consideration. From the uncertainty principle this distance is of the order of $\frac{1}{Q}$ where Q is the typical large transverse momentum in our experiment. E.g. in deeply inelastic electron scattering Q is the transverse momentum of the recoiled electron. We recall that deeply inelastic scattering is the reaction:

$$e + p \rightarrow e' + anything.$$

Thus, this reaction acts as a powerful microscope which is able to resolve the constituents of a hadron (quarks, antiquarks and gluons, collectively called partons) with a transverse size of the order of $\frac{1}{Q}$. The second kinematical variable that we can introduce for such constituents is the fraction of energy (x) that a parton carries with respect to the parent hadron. If $N(x, Q^2)dx$ is the number of gluons in a small x-interval centered around the value x at scale

Q^2 [3], the gluon density $xG(x,Q^2)$ tells us what the gluon density at a definite value of $\ln\frac{1}{x}$ is,

$$xG(x,Q^2) \;=\; |\frac{dN(x,Q^2)}{d\ln\frac{1}{x}}| \,.$$

Let us for convenience introduce the transverse density of gluons ρ,

$$\rho(x,Q^2) \;=\; \frac{xG(x,Q^2)}{\pi R^2} \tag{8}$$

where R is the radius of the hadron. We plot this on the vertical axis in Fig.4. In this figure we can see three different regions:

1. *The region of small ρ at small distances r (low density (pQCD) region).* This is the region where we can apply the powerful methods of perturbative QCD since the value of running coupling constant $\alpha_s(1/r^2)$ is small ($\alpha_s(1/r^2) \ll 1$).

2. *The region of large distances (npQCD region).* Here we have to deal with the confinement problems of QCD, since $\alpha_s(1/r^2) \gg 1$. In this kinematical region we need to use nonperturbative methods.

3 *The region of small distances but high parton density (hdQCD region).*

This is our region of interest, since here we have a unique situation when the coupling constant $\alpha_s(r^2)$ is still small but the density is so large that we cannot use the usual methods of perturbation theory. We have to think of something new in order to study this kinematical region. Already at this point we would like to point out that we can treat this region by approaching it from the low density pQCD region. The description of the methods developed to study this border region and the new physical phenomena that we anticipate there, are the main subjects of this review. Let us now examine each of these three regions in some more detail.

1.4 The low density (pQCD) region.

This is the region of small distance physics (corresponding to large values of transferred momentum Q^2 in processes such as deep inelastic scattering) and moderately small values of x. This is the workplace that the machinery of perturbative QCD described earlier was designed for. The physics for these so-called hard processes has some typical properties:

1. The cross section (e.g. for virtual photon absorption in deep inelastic scattering) is very small, $\sigma(\gamma^* N) \ll \alpha_{e.m.} \cdot \pi R_h^2$ where πR_h^2, is a typical area

[3] We will show later that the number of gluons increases in the region of small x. All physics in this kinematical region is strongly connected to this fact. It is the reason we concentrate on the discussion of the gluon density here

of the hadron. It decrease as the inverse power of Q^2 at large values of Q^2 ($\sigma(\gamma^* N) \propto \frac{1}{Q^2}$).

2. For these hard processes we have available a transparent physics language to discuss the relevant physics, viz. the parton language, which was especially conceived for these processes.

3. In this region, at truly large Q^2, one can apply the leading log approximation (LLA) of perturbative QCD.

Except at the Tevatron and HERA, all experiments checked mainly this kinematical region. In summary, one can say that the basics of QCD have been studied and confirmed experimentally during the last twenty years.

1.5 Nonperturbative QCD (npQCD) region.

In the kinematical region without a hard scale we also know a lot about QCD, mostly because of computer lattice calculations. This is perhaps the cheapest way to study the main properties of confinement of quarks and gluons starting directly from the QCD lagrangian. The success of this approach is quite remarkable. Lattice QCD is able to describe the spectrum of observed hadrons with an accuracy compatible with the experimental data (see the review of A.S. Kronfeld and P.B.Mackenzie [18] for a detailed discussion of all relevant problems). Unfortunately, at the moment lattice QCD cannot yet be applied to scattering processes. The same is true for another method which is not as general as the lattice approach but works for a large variety of processes in first approximation, the QCD sum rules [19]. They are roughly able to describe the property of confinement but this method uses the additional assumption that vacuum expectations of all operators are smaller in appropriate units than the typical hadronic scale (which is not always obvious). In spite of all these difficulties the situation in this kinematical region is not as bad as in the high density region of QCD.

1.6 High density QCD (hdQCD).

Here we are dealing with a system of partons still at short distances where the coupling constant of QCD α_s is small but in which the density of partons has become so large that we cannot apply the usual methods of pQCD. In essence the theoretical problem here is also a nonperturbative one but the origin of the nonperturbative effects here is quite different from that in the previous subsection. Here we face the situation where we have to develop new methods that let us deal with a dense relativistic system of gluons in a nonequilibrium state. Unfortunately we are only at the beginning of this road.

The best approach to this region is from the pQCD one. In some transition region on the border of the pQCD and hdQCD regions we can study this remarkable system of partons in great detail. To illustrate what new physics we can expect in this transition region let us consider deeply inelastic scattering in both regions. This we already did for the pQCD region in subsection 1.3.

In the transition region the situation changes crucially. First, the total cross section $\sigma(\gamma^* N)$ becomes large and, near the border with the so-called Regge domain, even compatible with the geometrical size of the hadron at small x, i.e. $\sigma(\gamma^* N) \to \alpha_{e.m.} \cdot \pi R_h^2$. In this kinematical region it depends only on $\ln Q^2$, that is $\sigma(\gamma^* N) \propto F(\ln Q^2)$. Second, the parton language can be used to discuss the main properties of this process but interactions between partons besides the ones due to the hard interaction, become important. This interaction induces substantial screening (a.k.a. shadowing) corrections. However, in this transition region the screening corrections are under some theoretical control. For this we must go beyond the usual linear evolution equation; the correct evolution equation becomes nonlinear. This we discuss in section 4. Next we consider how to experimentally access this transition region.

1.7 How to penetrate the high density QCD region.

Access to this interesting kinematical region is actually easily achieved in our scattering processes. We know at least three ways to prepare a large density system of partons. The first is given by nature, which supplies us with large and heavy nucleii. In ion-ion collisions we can already reach a very high density of partons at not so high energies, because the partons from different nucleons in a nucleus are freed. The second relates to hard processes in hadron-hadron collisions or in deep inelastic scattering. These also give us access to a high density of partons because we expect a substantial increase in the parton density in the region of small Bjorken x. Of course one can use hard processes in ion-ion collisions to utilize both effects: increase of gluon density combined with a large number of nucleons in a target. We will discuss these expectations in the next section. Let us remark that already the first experimental data from HERA [20] show that there are as many as 50 gluons in a proton at $x = 10^{-4}$. Yet another way to prepare a high parton density system is to select high multiplicity events in hadronic collisions. In the next section we will identify new physical phenomena which we expect to arise at small x_B.

2 New physical phenomena at small x_B:

Let us outline the new phenomena which we anticipate to occur in the region of small x_B in perturbative QCD for the case of deeply inelastic scattering. Three of them are particularly important and determine the physical picture of the parton evolution, or cascade as we shall call it, in the region of small x_B, namely:

1. The increase of the parton density [21] at $x_B \to 0$.

2. The growth of the mean transverse momentum of a parton inside the parton cascade at low x_B [21] [23].

3. The saturation of the parton density [23].

Before discussing each of these phenomena in turn, let us try to understand these new phenomena at small x_B by recalling some facts regarding perturbation theory and deeply inelastic scattering. According to the factorization theorem, the deep-inelastic structure function is a product of a parton density and a short distance coefficient function, which is calculable in perturbation theory. Both factors depend on the factorization scale, which we choose equal to Q^2. Concentrating on the gluon density, in the kinematical region we are considering the former can be represented as

$$xG(x,Q^2) = \Sigma_n C_n(Q_0^2)(\alpha_s L)^n \; + \; O(\alpha_s(\alpha_s L)^n) \; , \tag{9}$$

where L is the large logarithm in our problem. The coefficients $C_n(Q_0^2)$ contain nonperturbative information and depend on the initial scale Q_0^2 of the cascade, see Fig.5,

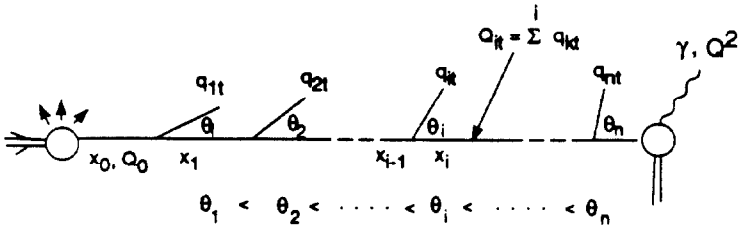

Figure 5: The basic branching process in deep-inelastic scattering.

To see what kind of large logarithm could occur, one can examine the probability of emission P_i of the i-th parton in the cascade. Near $x = 0$ it can be written as

$$P_i = \frac{N_c \alpha_s}{\pi} \cdot \frac{dx_i}{x_i} \cdot \frac{dq_{it}^2}{q_{it}^2}$$

1. In the region of large virtualities of the photon in deep inelastic scattering (but not at very small values of x_B) L is equal to $\ln Q^2$.

2. At Q^2 fixed ($Q^2 \simeq Q_0^2 \gg m^2_{proton}$) but at small value of x_B we have a different large logarithm in eq.(2), namely $L = \ln \frac{1}{x_B}$.

3. When both $\ln Q^2$ and $\ln \frac{1}{x_B}$ are large ($Q^2 \gg Q_0^2$ $x_B \to 0$) the large logarithm has a more complicated form, namely $L = \ln Q^2 \ln \frac{1}{x_B}$. In this case one can apply the so-called double logarithmic approximation (DLA) of pQCD. The objective now is to resum these large logarithms in eq.(9), so that we can estimate the behavior of the parton densities in the corresponding kinematical regimes. This resummation is performed via evolution equations, which differ depending on the type of large logarithm under consideration.

2.1 Increase of the gluon (quark) density at $x_B \to 0$.

We now investigate the new phenomena at small x_B, but begin by discussing the evolution equations that sum particular classes of large logarithms in the parton densities.

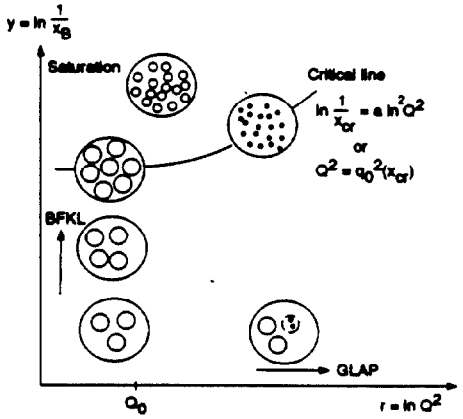

Figure 6. The parton distribution in the transverse plane.

Gribov - Lipatov - Altarelli - Parisi (GLAP) evolution equation.

The GLAP equation sums those contributions in the parton cascade which compensate the smallness of the QCD coupling constant α_s by the large logarithm $\ln Q^2$. It reads

$$\frac{d}{d\ln Q^2}\phi(x,Q^2) = \alpha_s(Q^2)\int_x^1 \frac{dz}{z}P(z)\phi(\frac{x}{z},Q^2)$$

where $P(z)$ is the Altarelli-Parisi evolution kernel, calculable in perturbation theory, and $\phi(x,Q^2)$ is a generic parton density (matrix).

Clearly, from the expression for P_i, we need strong ordering ($Q^2 \gg ... \gg q_{it}^2 \gg ..... \gg \frac{1}{R_p^2} = Q_0^2$) in transverse momenta of emitted partons since only under such a condition does one get a $\ln Q^2$ contribution for each integration over q_{it} in the parton cascade in Fig.5. This strong ordering means that the GLAP evolution equation allows us to calculate the probability to find a parton of transverse size $r_t \approx \frac{1}{Q}$ inside the initial parton (quark or gluon) in the hadron at fixed x_B. In the case where both Q^2 and $1/x_B$ are very large (the DLA approximation), the AP kernel simplifies to $P(z) = N_c\alpha_s/\pi z$, and the solution to the GLAP equation for the gluon density reads then

$$xG(x,Q^2) \sim xG(\omega_0, Q_0^2)\ \exp(\sqrt{\frac{4N_c\alpha_s}{\pi}\ln\frac{Q^2}{Q_0^2}\ln\frac{1}{x}})\sqrt{\frac{\omega_0^3}{3\alpha_s\ln\frac{Q^2}{Q_0^2}}},$$

where $\omega_0 = (\frac{N_c\alpha_s}{\pi}\ln\frac{Q^2}{Q_0^2}/\ln\frac{1}{x})^{1/2}$, and Q_0 is the initial scale of the parton cascade.

Note that the solution of the GLAP equation decreases as Q^2 increases. This agrees with the intuitive notion that, because of asymptotic freedom, the hadron should be almost empty at small distances.

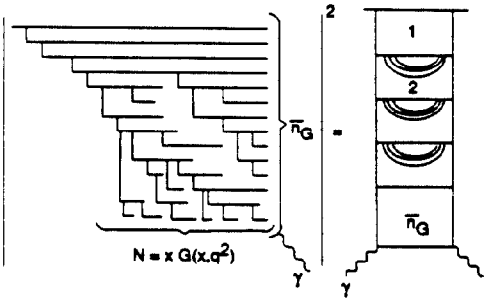

Figure 7. Structure of the parton cascade at small x_B and the coherence in the ladder diagram.

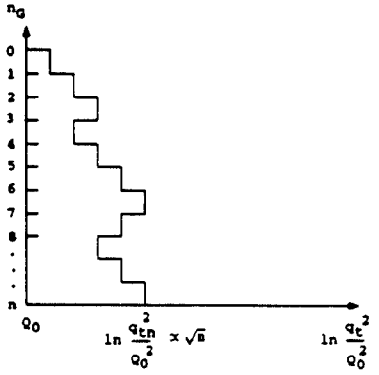

Figure 8. The random walk picture in $\ln q_t^2$.

Balitski- Fadin -Kuraev - Lipatov (BFKL) evolution.

The situation changes crucially if we consider the behavior of the parton density ϕ in another extreme regime: at fixed Q^2 but small x_B. Here we have the large logarithm $L = \ln \frac{1}{x_B}$. The picture of the parton cascade, Fig.7, shows that the number of partons increases drastically in the region of small x_B, since each parton in the basic branching process in Fig.5 is allowed, due to the abundance of available energy, to decay in its own chain of daughter partons. Let us estimate the total multiplicity of gluons N_G associated with this complicated process.

We are able to estimate the number of cells in this chain diagram, which corresponds to the typical number of parton (gluon) emissions in one *sub*process in our parton cascade ($\overline{n_G}$). The characteristic value of $\Delta y_{i,i+1}$, the rapidity difference between two adjacent rungs of the ladder, is equal to $\Delta y_{i,i+1} \propto 1/\alpha_s$, from the expression for gluon emission P_i. Thus

$$\overline{n_G} = \frac{\ln \frac{1}{x_B}}{\Delta y_{i,i+1}} \propto \alpha_s \cdot \ln \frac{1}{x_B} . \tag{10}$$

The total number of N_G partons that could interact with the target can then be calculated as follows (see Fig.7):

$$N_G \propto e^{\overline{n_G}} = e^{c\alpha_s \ln 1/x_B} = (\frac{1}{x_B})^{c\alpha_s} , \tag{11}$$

where the constant c should be calculated using the exact BFKL equation [21]. In first approximation $c\alpha_s = 0.5$.

2.2 A new scale for the deeply inelastic process at $x_B \to 0$.

Thus in the region of small x_B the density of partons increases. A careful study of the behavior of the parton cascade shows that also the mean transverse momentum of the parton increases. The reason is as follows. In the case where we neglect the running coupling constant of QCD our theory is dimensionless so each emission leads to a value of the transverse momenta of the daughter gluons which is of the same order as the transverse momentum of the parent gluon. This could be seen just from the explicit expression of P_i. We introduce the ratio $|\ln q_{i,t}^2/q_{i+1,t}^2|$ which characterizes the emission. It is roughly constant. After n_G emissions

$$< |\ln(q_{n,t}^2/Q_0^2)| > \propto \sqrt{n_G} \approx \sqrt{\alpha_s \ln \frac{1}{x_B}} , \tag{12}$$

since the parton cascade corresponds to a random walk in the variable $\ln(q_{n,t}^2/Q_0^2)$ [21][63] (see Fig.8). The new scale mentioned in the title of this subsection is $q_{n,t}^2$.

Although we will not explicitly present the BFKL equation here, we will give the solution to this equation with the initial condition $x_B G(x_B = x_0) = \delta(\ln(Q^2/Q_0^2))$. This is instructive because it shows explicitly all the properties mentioned in the above:

$$G(y-y_0, r-r_0) = \sqrt{\frac{Q^2}{Q_0^2}} \cdot \frac{1}{\sqrt{\pi \Delta \omega (y-y_0)}} \cdot \exp\{\omega_0 (y-y_0) - \frac{(r-r_0)^2}{8\Delta\omega_0 (y-y_0)}\}$$

where

$$\omega_0 = \frac{\alpha_s(Q_0^2) N_c}{\pi} 4\ln 2, \ \Delta = \frac{14\zeta(3)}{4\ln 2}, \ y - y_0 = \ln\frac{x_0}{x_B}, \ r - r_0 = \ln\frac{Q^2}{Q_0^2}$$

2.3 Saturation of the gluon density.

The increase of the parton density leads to a new problem in deeply inelastic scattering, namely the violation of s-channel unitarity. This is the requirement that the total cross section for virtual photon absorption be smaller than the size of a hadron.

$$\sigma(\gamma^* N) \ll \pi R_h^2 \tag{13}$$

At small x_B the gluon density dominates and we can write

$$\sigma(\gamma^* N) \ = \ const \frac{\alpha_{em}}{Q^2} \ xG(x, Q^2) \tag{14}$$

where *const* α_{em}/Q^2 approximates the cross section $\sigma(\gamma^* g)$. We have shown previously that the value of the gluon density increases very rapidly as $x \to 0$. Using the DLA result (see eq.(11)), we can rewrite the unitarity constraint in the following way, dropping the *const*:

$$\frac{\alpha_s(Q^2)}{Q^2} \cdot (\frac{1}{x_B})^{c\alpha_s(Q^2)} \leq \pi R_N^2. \tag{15}$$

Here we replaced α_{em} by α_s since the probe can also be a virtual gluon, not just a virtual photon.

From this expression alone one can conclude that **unitarity will be violated** [23] at

$$x < x_{\rm cr} \ \text{ where } \ \log\frac{1}{x_{\rm cr}} \ = \ \frac{1}{c} \cdot \frac{1}{\alpha_s(Q^2)} \ln(\frac{\pi R_N^2 Q^2}{\alpha_s(Q^2)}) \tag{16}$$

Therefore unitarity is violated even for (very) large values of Q^2 when $x < x_{\rm cr}$. Clearly the miraculous confinement force cannot prevent this from happening. Thus we have to look for the origin and solution of this problem within pQCD.

Let us try to understand what happens in the region of small x_B by examining the parton distribution in the transverse plane (see Fig.6) [4]. Our probe (photon) feels those partons whose size is of the order of $\frac{1}{Q}$. To begin, at $x \sim 1$ we have only several partons that are distributed in the hadronic disc. If we choose Q^2 such that

$$r_p^2 \approx \frac{1}{Q^2} \ll R_h^2. \tag{17}$$

then the distance between partons in the transverse plane is much larger than their size and we can neglect the interaction between partons. The only process which is essential here is the emission of partons that is taken into account in the usual evolution equation. As x decreases the number of partons increases and at some value of $x = x_{\rm cr}$ partons start to densely populate the whole hadron disc. For $x < x_{\rm cr}$ the partons overlap spatially and begin to interact throughout the disc. For such small x-values the processes of recombination and annihilation of partons should be as essential as their emission. Both these processes are however not incorporated into either the GLAP or BFKL evolution equations.

What happens in the kinematical region $x < x_{cr}$ is anybody's guess but there is enough experience with some models [24] to suggest the so-called **saturation of the parton density** [3]. This means that the parton density ϕ, which we discussed before, is constant in this domain.

3 Two scales of hardness at high energy.

3.1 Two scales of hardness for deeply inelastic processes.

Let us now discuss all new phenomena on a more quantative basis starting from the low density (pQCD) region. First, we need to incorporate in our theoretical approach the increase of the gluon density and the gluon mean transverse momentum. For simplicity, to illustrate all problems encountered in the region of large energy (small x_B), let us consider again deeply inelastic scattering.

The main difference between the small x_B region and the region of moderate x_B comes from the fact that we have **two scales of hardness** in deeply inelastic scattering, namely Q^2 and the mean transverse momenta of the emitted gluons $\langle p_t^2 \rangle$. Thus we cannot use the GLAP evolution equation. Rather, we should first of all study what scale is important in the region of small x_B.

In ep scattering we can distinguish three different regions in this process where the different scales of hardness are relevant.

[4] Recall that a high energy hadron in the parton model can be represented as a Lorentz contracted disc.

1. If Q^2 is larger than the mean transverse momentum of gluon $\langle p_t^2 \rangle$ the hard cell of our process consists of the exchange of the virtual photon (see Fig.9). In this case we have a typical deeply inelastic process and we can use the GLAP evolution equation.

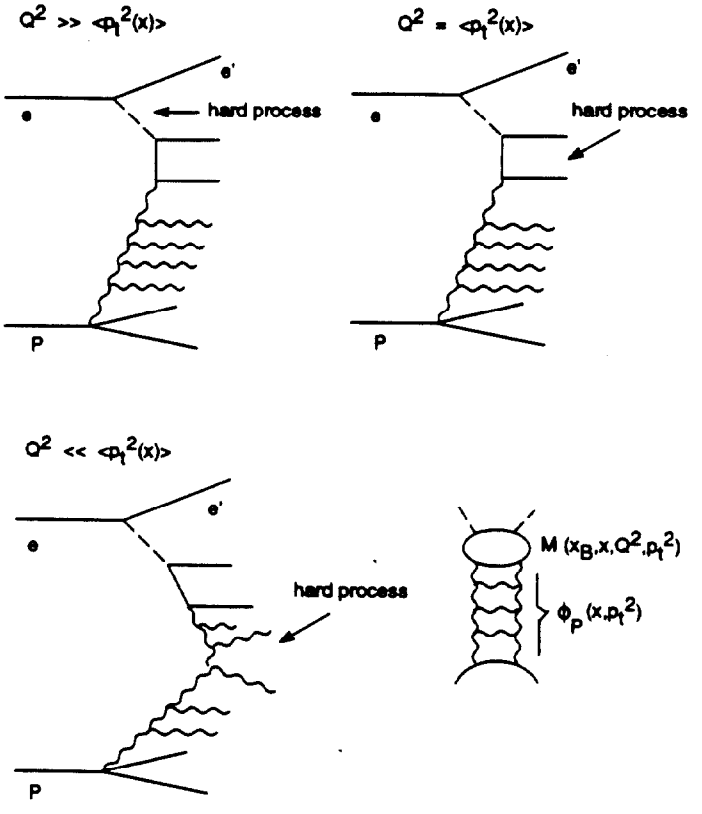

Figure 9. Deep-inelastic scattering in different kinematic regimes; $< p_t >$ is the mean transverse momentum of the gluon.

2. If Q^2 is of the order of $\langle p_t^2 \rangle$ we have to calculate the interaction of the gluon with the virtual photon more accurately since it is this interaction that tells us what scale is important in this kinematic region and what the relevant hard process (hard cell) is. E.g. it could be quark - antiquark production rather than the exchange of a virtual photon. However, we know how to calculate the deep inelastic process in this region. The correct amplitude $M(x_B, x, Q^2, p_t^2)$, also depicted in Fig.9, was calculated in refs. [10]. Thus in this kinematical region we need to improve the GLAP equation. This was done in [25]. Here the emission of a parton in the basic branching process (Fig.1) was rewritten

in a form such that it depends only on the previous stage of emission. Such a form is very well suited for Monte-Carlo simulations and allows one to obtain a numerical solution for the evolution of the parton cascade.

3. For the case $\langle p_t^2 \rangle \gg Q^2$ the hard cell is somewhere in the middle of our parton chain, Fig.9. This means that in this kinematical region the deeply inelastic process looks rather more like high q_t jet production in hadron- hadron collisions than a probe of the parton content of the target nucleon. All ingredients, e.g. to determine the (off-shell) photonic parton densities, are present for a thorough investigation of this process. However this has not been done yet.

3.2 Transverse momentum factorization.

A natural generalization of eq. (7) is so-called transverse momentum factorization [10]. The transverse momentum factorization generalizes the factorization theorem (7) to the case when the value of the mean transverse momentum of partons becomes compatible with the natural scale of hardness in the process, e.g. the k_t of a produced jet. It reads (for inclusive one-jet production)

$$\frac{d\sigma(A+B \to jet(x_j,k_t)+X)}{d\ln x_j d^2k_t} = \sum_{ab} \int dx_a dx_b d^2k_{ta} d^2k_{tb} \qquad (18)$$

$$\Phi_{a/A}(x_a,k_{ta})\Phi_{b/B}(x_b,k_{tb})\mathcal{I}(x_a x_b s, k_{ta}^2, k_{tb}^2, k_t^2)\delta^{(2)}(\mathbf{k_t} - \mathbf{k_{ta}} - \mathbf{k_{tb}}) \ .$$

where A and B are hadrons, x_j is the longitudinal momentum fraction of the jet and the Φ are so-called unintegrated parton densities: $\int_0^{\mu^2} dk_t^2 \alpha_s(k_t^2)\Phi(x,k_t^2) = \alpha_s(\mu^2)\phi(x,\mu^2)$. Furthermore, $\mathcal{I}$ is the so-called impact factor which represents the cross section of "hard" scattering of off-shell partons. The impact factor has been calculated for many reactions in refs. [10]. For gluon jet production it looks quite simple:

$$\mathcal{I} = \frac{3N_c}{\pi k_t^2}\alpha_s(min\{k_{ta}^2, k_{tb}^2, k_t^2\}) \ .$$

In eq.(18) we can distinguish three kinematical regions:

1. $k_{ta} \sim k_t \gg k_{tb}$. Here the gluon jet production can be rewritten in the form:

$$\frac{d\sigma(A+B \to jet(x_j,k_t)+X)}{d\ln x_j dk_t^2} = \sum_{ab} \int dx_a dx_b \frac{3N_c\alpha_s(k_t^2)}{\pi k_t^2} \qquad (19)$$

$$\frac{dx_a\phi_{a/A}(x_a,k_t^2)}{dk_t^2} x_b\phi_{b/B}(x_b,k_t^2) \ .$$

2. $k_{tb} \sim k_t \gg k_{ta}$.

Obviously we obtain the same expression as in the previous kinematical region via the substitution $A(a) \to B(b); B(b) \to A(a)$. The above two regions together yield a simple formula for inclusive gluon jet production which is a direct consequence of the ordinary factorization formula (7) with the particular scale choice $\mu = k_t$:

$$\frac{d\sigma(A+B \to jet(x_j,k_t)+X)}{d\ln x_j dk_t^2} = \sum_{ab}\int dx_a dx_b \frac{3N_c\alpha_s(k_t^2)}{\pi k_t^2} \frac{d[x_a\phi_{a/A}(x_a,k_t^2)\cdot x_b\phi_{g/B}(x_b,k_t^2)]}{dk_t^2} . \tag{20}$$

As far as we know this formula was first proposed by Blaizot and Mueller [28].

3. $k_{ta} \sim k_{tb} \gg k_t$.

The transverse momentum factorization formula takes into account this kinematic region which is completely omitted in the approach based on the ususal factorization theorem. In this kinematic region the total inclusive cross section cannot be deduced from the usual factorization formula (see eq.(7)) and has the form:

$$\frac{d\sigma(A+B \to jet(x_j,k_t)+X)}{d\ln x_j dk_t^2} = \sum_{ab}\int dx_a dx_b \frac{3N_c\alpha_s(k_t^2)}{\pi k_t^2} \int_{k_t^2} dk_t'^2\, \Phi_{a/A}(x_a,k_t'^2)\cdot\Phi_{b/B}(x_b,k_t'^2) . \tag{21}$$

Note that this region corresponds to a final state high parton density problem.

3.3 Small k_t behavior of the one-jet inclusive cross section and Landau - Pomeranchuk suppression.

Inspecting the formulae for inclusive one-jet production one notes that this cross section becomes very large at small values of k_t ($\frac{d\sigma}{dk_t^2} \propto \frac{1}{k_t^2}$). The physical meaning of this behavior is easily understood by recalling that the *total* inclusive cross section yields essentially the multiplicity of produced jets, which is very large at small values of the transverse momenta. Thus in order to understand the small-k_t behavior of this process we have to deal with a high density parton system even if the initial energy is not very high. Of the three kinematical regions defined in the previous subsection, it is very instructive to consider the first two separately from the third since then the low k_t behavior is caused by different physics.

In the first two kinematic regions it is the behavior of the gluon density (xG) that governs the behavior. Indeed, at small-k_t the gluon density is proportional to k_t^2, due to gauge invarience of QCD. When x_j is not too small the scale of such behavior μ ($xG \propto \frac{k_t^2}{\mu^2}$) is defined by confinement and cannot be calculated in the framework of perturbative QCD. However at high energy (small x_j) μ is just the new scale $q_0(x_j)$ originated by the saturation of the gluon density, see Fig.6. Thus at small x_j, and at a small value of the transverse momentum of the produced gluon, the one jet inclusive production in the first two kinematic regions can be written as

$$\frac{d\sigma(A+B \to jet(x_j,k_t)+X)}{d\ln x_j d^2k_t^2} \;=\; 2\,\frac{3N_c\alpha_s(k_t^2)}{\pi}\Phi_0(g/A)\Phi_0(g/B)\,, \qquad (22)$$

where ϕ_0 is the limiting value of gluon density that we have discussed in section 2.3. We will consider it in more detail in the next section.

However, even the saturation hypothesis cannot help us determine the final value of the inclusive cross section at small-k_t for the third kinematic region (see eq.(21). This is because this region describes gluon production in the *final state.*

Here we need to invoke the so-called Landau-Pomeranchuk effect ref.[29], which has been studied in detail in QED [30] and has been reproduced in QCD [31]. The essence of the LP effect is that if the formation time (τ) of photon (gluon) emission becomes larger than the mean free path in the medium (λ), destructive interference occurs between radiation amplitudes associated with multiple collisions in the medium. This suppresses the photon (gluon) bremsstrahlung. The formation time τ is the minimal time needed to resolve the transverse wavepacket of a quantum with $\Delta x_\perp \sim 1/k_\perp$ from the wavepacket of its high energy (E) parents (E $\gg \omega$ where ω is the photon (gluon) energy). The photon (gluon) emitted at angle $\theta = \frac{k_\perp}{\omega}$ moves in a transverse direction a distance $b_\perp = \theta\tau$ during time τ. The photon (gluon) can be resolved only if $b_\perp \geq \Delta x_\perp \sim \frac{1}{k_\perp}$. This inequality gives for the formation time. $\tau \propto \frac{\omega}{k_\perp^2} = \frac{1}{m_p x_B}$ where m_p is the proton mass. The Landau-Pomeranchuk effect can be understood in a simpler way in QCD than in QED since in QCD each gluon exchange leads to a change of the color of the emitted gluon and therefore destroys the coherence of the emission. If $c\tau \gg \lambda$ the process of emission becomes noncoherent. It can be divided in $n = c\tau/\lambda$ intervals between which there is no coherence, due to destructive interference between these intervals, so that the cross section is proportional rather to n than to n^2, as is the case of coherent emission, usually called bremsstrahlung. Finally we have to multiply eq.(21) by a factor C. A simple interpolation formula for C that describes two

regimes, coherent and completely incoherent emission, looks as follows:

$$C = \frac{\lambda}{\lambda + c\tau} . \tag{23}$$

This formula gives suppression of emission that leads to the final value of the inclusive cross section both at small x_j and at small k_t, since $\lambda \propto k_t^2$ while $\tau = 1/m_p x_j$.

Unfortunately we have no space to discuss the physics of the LP effect so we have to refer to theoretical paper on QED and QCD LP effect [29] [30][31]. The QED LP effect has been studied experimentally recently at SLAC, [32]. It shows excellent agreement with theory. However, much more experimental work is needed to check the applicability of this method to control the accuracy of our calculation in the case of QCD. Let us finally remark that the LP effect in the context of the factorization theorem means that in this kinematic region the leading-twist factorization theorem (7) no longer applies since we have to take into account higher twist contributions which are intimately related to rescattering of produced partons (quark or/and gluon) in the environment of a relatively dense parton cloud.

3.4 Parton cascade in real time.

Let us briefly mention a different approach to the calculation of inclusive production. It was first suggested by Blaizot and Mueller [28] and was carried significantly further by Geiger and Muller [33] (see also Geiger's paper [34]).

The main idea rests on the fact that the simple factorization formula, eq.(20), is correct in the very instant of the first collision ($t = t_0$) between partons from different hadrons, which results in production of a jet with kinematic variables (x_j, k_t). Thus we can use formula (20) as the initial condition at $t = t_0$ for the evolution of the final state parton cascade.

We can write the semiclassical transport equation for this evolution (see refs.[28][33][34] for details) introducing the time-dependent spatial density of partons of species a $F_a(\mathbf{p}, \mathbf{r}, t)$, where $F_a d^3p d^3r$ is the expected number of partons of type a in d^3r about $\mathbf{r}$ with momentum d^3p about $\mathbf{p}$ at time t.

The transport equation can be written in the form:

$$p^\mu \partial_\mu F_a = \sum_{processes} I , \tag{24}$$

where I is the Lorentz invariant collision integral. The exact form of I one can find in refs.[33],[34]. The gluon density can then be written as

$$xG(x, k_t^2) = \int_0^{k_t^2} dk_t'^2 d^3r F_G(k_t', k_z, r, t = 0) . \tag{25}$$

We can use the above expression together with eq.(20) to establish the initial condition for the transport equation. Unfortunately, such an initial condition has not been used in practical applications of the method (see refs. [33][34]).

In such an approach we hide all the problems of small transverse momentum behavior as well as the violation of the factorization theorem in the concrete form of the collision integral in the transport equation. It is the most economic way for writing Monte Carlo programs that simulate the structure of the final state in a typical inelastic event. However it is very difficult to take into account coherence effects such as the LP effect. Without taking this into account however we certainly overestimate the number of partons in the final state. E.g. we then cannot perform a reliable evaluation of the probability for Quark Gluon Plasma production in ion-ion collisions, in the case where we are dealing with a dense system of produced partons.

4 Shadowing corrections and nonlinear evolution equation.

4.1 Qualitative derivation of nonlinear (GLR) evolution equation

We have discussed in section **2.3** that at small x_B (high energies) the density of gluons becomes so large that the unitarity constraint is violated, even at large values of Q^2. We argued that the physical processes of interaction and recombination of partons, which are usually omitted in perturbative calculations, become important in the parton cascade at a large value of the parton density. To take into account such processes we have to identify a new small parameter that lets us estimate the accuracy of our calculations. This small parameter is [23]

$$W = \frac{\alpha_s}{Q^2}\,\rho(x,Q^2)\,. \tag{26}$$

The first factor in eq.(26) is the cross section for gluon absorption by a parton from the hadron, whereas ρ is defined in (8). Effectively, W is the probability of a parton (gluon) recombination in the parton cascade. We can rewrite the unitarity constraint (15) in the form

$$W \leq 1\,. \tag{27}$$

Thus, W is the natural small parameter in our problem. Amplitudes which take gluon recombination into account can be expressed as a perturbation series in this parameter [23]. We can resum this series, and the result of the resummation

[23] can be easily understood by considering the structure of the QCD cascade in a fast hadron. Inside the cascade there are two processes that occur

$$\text{Emission } (1 \to 2); \quad \text{Probability } \propto \alpha_s \rho \ ; \tag{28}$$

$$\text{Annihilation } (2 \to 1); \quad \text{Probability } \propto \alpha_s^2 r^2 \rho^2 \ \propto \ \alpha_s^2 \frac{1}{Q^2} \rho^2 \ ,$$

where r is the size of produced parton in the annihilation process. For deep inelastic scatterinq $r^2 \propto \frac{1}{Q^2}$.

It is obvious that at $x_B \sim 1$ only the production of new partons (emission) is essential since $\rho \ll 1$, but at $x_B \to 0$ the value of ρ becomes so large that the annihilation of partons enters into the game. This simple parton picture then allows us to write an equation for the density of partons, ρ, that takes all these processes properly into account. The number of partons in a phase space cell $(\Delta y = \Delta \ln \frac{1}{x_B}, \Delta \ln Q^2)$ increases due to emission and decreases as result of annihilation and thus the balance equation reads

$$\frac{\partial^2 \rho}{\partial \ln \frac{1}{x_B} \partial \ln Q^2} = \frac{\alpha_s N_c}{\pi} \rho - \frac{\alpha_s^2 \gamma}{Q^2} \rho^2 \ , \tag{29}$$

or in terms of the gluon structure function $x_B G(x_B, Q^2)$

$$\frac{\partial^2 x_B G(x_B, Q^2)}{\partial \ln \frac{1}{x_B} \partial \ln Q^2} = \frac{\alpha_s N_c}{\pi} x_B G(x_B, Q^2) - \frac{\alpha_s^2 \gamma}{\pi Q^2 R^2} (x_B G(x_B, Q^2))^2 \ . \tag{30}$$

This is the so-called GLR equation [23]. The parameter γ can in fact be calculated order by order in W-perturbation theory, and was found in ref.[35] to be

$$\gamma = \frac{81}{16} \quad \text{for } N_c = 3.$$

4.2 The scale of the shadowing corrections (SC).

The second term in eq.(30) describes the shadowing corrections and its value crucially depends on the value of R^2. The physical meaning of R^2 is clear: R is the correlation radius between two gluons in a typical hadronic situation (at $x_B \sim 1$). In our derivation of the GLR equation we made the assumption that there are no correlations between gluons except due to the fact that they are confined in a disc of radius R.

If $R = R_{proton}$ the value of the SC is negligably small.

If $R \ll R_{proton}$, the SC could be large (see refs. [41][42][46]). Recently the first theoretical estimates of the value of R have been performed by Braun et al. [43] within the framework of QCD sum rules. They found

$$R \;=\; 0.3 - 0.35\,Fm \;\sim\; \frac{1}{3}\,R_{proton}\;.$$

an encouraging result for experimental study of SC at present energies.

4.3 New scale of transverse momentum (the critical line).

4.3.1 The main property of a solution of the GLR equation

First let us rewrite the GLR equation eq.(30) in new variables: $F = xG(x,Q^2)$; $y = \frac{8N_c}{b}\ln\frac{1}{x_B}$ and $\xi = \ln\ln Q^2/\Lambda^2$. In these variables it reads:

$$\frac{\partial^2 F}{\partial y \partial \xi} \;=\; \frac{F}{2}\cdot\{1 \;-\; \gamma' exp[-\xi \;-\; e^{\xi}]\,F\}\;, \tag{31}$$

where $\gamma' \;=\; \frac{2\pi\gamma}{bR^2\Lambda^2}$ and the terms e^{ξ} $(\,-\xi)$ in the exponent correspond $\frac{1}{Q^2}$ (α_s) resp. Inspecting eq.(31) we can guess the main property of the solution. At the start of the evolution when the value of the structure function is small we can neglect the nonlinear term. The derivative with respect to y is positive here, so the structure function increases monotonically with y, or $\ln\frac{1}{x}$. This growth continues up to the value

$$F_{max} \;=\; \frac{1}{\gamma'}\cdot exp[\xi \;+\; e^{\xi}]\;.$$

At this value of F the derivative vanishes. If $F > F_{max}$ the derivative from the GLR equation becomes negative and thus F_{max} is the limiting value of the gluon density and is the solution of the GLR equation as $x \to 0$.

Therefore, at each value of Q^2 there is a critical value of $x = x_{cr}$ when $F = F_{max}$ or, conversely, at each value of x there is a critical value of $Q^2 \;=\; q_0^2(x)$ when $F = F_{max}$. This value $Q^2 = q_0^2(x)$ is a new scale of transverse momentum in the parton cascade. The behavior of the gluon density changes crucially at $Q^2 = O(q_0^2(x))$. Indeed:

$$Q^2 \;>\; q_0^2(x) \qquad F = F^{GLAP}(x, \ln Q^2)\;,$$

where F^{GLAP} means that F is a solution of the linear GLAP equation and a smooth function of $\ln Q^2$. Alternatively

$$Q^2 \;<\; q_0^2(x) \qquad F \;\propto\; \frac{Q^2}{q_0^2(x)}\cdot F_{max}\;.$$

We postpone the discussion of the physical meaning of this new scale and instead determine first the x dependance of $q_0^2(x)$.

4.3.2 Trajectories.

To study the solution of the GLR equation it is very useful to start with a semiclassical approach which based is on so called trajectories. It is easiest to find the solution to the linear equation by passing to a moment (ω) representation and introducing the anomalous dimension γ. In moment representation the solution then looks as follows:

$$F(x,Q^2) \;=\; \int \frac{d\omega}{2\pi i} M_0(\omega,Q^2) e^{\omega y \,+\, \gamma(\omega)\xi} \;, \tag{32}$$

where $M_0(\omega,Q^2)$ is the initial distribution at $Q^2 = Q_0^2$ and the anomalous dimension $\gamma(\omega) = \frac{1}{2\omega}$. At large y (small x) we can perform the integral by saddle point approximation. The position of the saddle point is determined by:

$$y \;=\; -\frac{d\ln M_0(\omega)}{d\omega} \;-\; \frac{d\gamma(\omega)}{d\omega}\cdot\xi \;. \tag{33}$$

This equation describes a family of curves $x = x(\xi)$ which can be considered as semiclassical trajectories of parton evolution, since ω is a constant of a motion in the linear evolution equation. The semi-classical values of (y,ξ) along the trajectory give an approximate estimate of the structure function at fixed Q^2 and x. Of course this method yields nothing new for the linear equation, however it can be generalized to the nonlinear case.

4.3.3 Semi-classical solution to the GLR equation.

In semi-classsical approximation we parametrize the solution to the GLR equation by writing

$$F \;=\; e^S \quad \text{assuming } S_y\, S_\xi \;\gg\; S_{y\xi} \;,$$

where $S_y = \frac{\partial S}{\partial y}$, $S_\xi = \frac{\partial S}{\partial \xi}$ and $S_{y\xi} = \frac{\partial 2S}{\partial y \partial \xi}$. It should be noted that for the linear equation $S = \sqrt{2y\xi}$ and one can check that the above inequality holds to good accuracy.

Thus in the semiclassical case the GLR equation can be reduced to the form:

$$S_y\, S_\xi \;=\; \frac{1}{2}(1 \;-\; \gamma'\, exp\{\, S \;-\; e^\xi \;-\; \xi\,\}) \;. \tag{34}$$

Eq. (34) can be solved with the method of characteristics, or trajectories [23], [45], [44]. Introducing the "intrinsic" time along the trajectory and denoting

the derivatives with respect to this time variable by $\dot{y}$ etc. we can rewrite the GLR equation as the following system of ordinary equations:

$$\begin{aligned} \dot{y} &= S_\xi \\ \dot{\xi} &= S_y \\ \dot{S} &= 2\,S_y\,S_\xi \\ \dot{S}_y &= -\gamma'\,S_y\,exp\{\,S\,-\,e^\xi\,-\,\xi\,\} \\ \dot{S}_\xi &= -\gamma'\,[\,S_\xi\,-\,1\,-\,e^\xi\,]\,exp\{\,S\,-\,e^\xi\,-\,\xi\,\}\,. \end{aligned} \tag{35}$$

In the linear case this system of equations has simple solution:

$$S_y = \omega = Const\;;\;\; S_\xi = \frac{1}{2\omega} = Const\;,$$

which coincides with eq.(33). Along each trajectory of the linear equation the rescattering probability $W = \gamma' exp\{S - e^\xi - \xi\}$ increases at the beginning when $\dot{S} \approx 1$, reaches the maximum value when $S_\xi = (1 + e^\xi)$ and then decreases at larger ξ. However the trajectories of the GLR equation become quite different from the linear ones. Indeed, in the region where W becomes of order one the derivatives S_y and S_ξ are not small and trajectories are not straight lines. It has been shown in a number of papers ([23] [45] [44]) that a remarkable trajectory (critical line) exists in the nonlinear equation that separates the region of almost linear trajectories (small values of $W \leq 0(\alpha_s)$) and strong nonlinear solutions.

It is easy to check explicitly that for large ξ

$$y_{cr} = \frac{e^{2\xi}}{4}\;;\;\; S = e^\xi\,-\,\ln\gamma'\;;\;\; S_y = e^{-\xi}\;;\;\; S_\xi \approx \frac{e^\xi}{2} \tag{36}$$

is the solution of eq.(35) and the GLR equation as well. To the right of the critical line ($x > x_{cr}$) the equation $y_{cr} = \frac{e^{2\xi}}{4}$ looks as follows in the usual notation:

$$\ln\frac{1}{x_{cr}} = \frac{b}{32N_c}\ln^2(Q^2/\Lambda^2) \tag{37}$$

the nonlinear corrections are so small that we can neglect them and can use the trajectory of the standard GLAP equation. However when x becomes smaller than x_{cr}, $w \to 1$ and we have to use the nonlinear trajectory. The remarkable fact is that trajectory cannot cross the critical line which is also a trajectory. Using this property one can suggest the following way to solve the GLR equation. To the right of the critical line it is enough to find the solution of the linear (GLAP) equation with the new boundary condition $F = e^S$ with $S = e^\xi - ln\gamma'$

on the critical line (see eq.(36)). To the left of the critical line we have a separate system of trajectories. The solutions to the left do not depend on the solutions to the right of the critical line. However precisely here we enter the very interesting kinematic region of *high density QCD*. Even the GLR equation is not the right tool to solve problems in this region since not only the recombination of two partons is important in this region but also simultaneous interaction of three, four and etc partons.

4.4 The physical meanning of new scale for the typical transverse momentum in the parton cascade.

The equation for the critical line (37) yields a new scale for the value of the typical transverse momentum in our parton cascade, namely:

$$q_t^2 \;=\; q_0^2(x)\,|_{x\to 0} \;\to\; \Lambda^2\, e^{\sqrt{\frac{32N_c}{b}\,\ln\frac{1}{x}}}\,. \tag{38}$$

In section 3.3 we have argued that this new scale plays the role of the infrared cut-off in inclusive production (see eq. (20)). It should be stressed that this new infrared cut-off has a dynamical origin: parton - parton recombination in the parton cascade. It is not related to confinement.

We would like to draw attention to the fact that $q_0(x)$ is also the Landau-Pomeranchuk momentum in our parton medium. Indeed, in the saturation region $q_t < q_0(x)$ the mean free path λ does not depend on x. $\lambda = 1/\sigma T$ where σ is cross section of parton - parton interaction ($\sigma \propto \alpha_s \frac{1}{q_t^2}$) and $T = xG(x,q_t)$ is the number of partons with transverse momentum q_t at fixed x. If $q_t < q_0(x)$ $T \propto q_t^2\phi_0$ and $\sigma T = Const(q_t)$. Thus λ is equal to the formation length of a parton with $x = x_0$ that can be found from the relation $q_0(x_0) = q_t$. If $q_t > q_0(x)$ then $\sigma T \propto xG(x,q_t)/q_t^2 \ll 1/mx$ so λ is big. Therefore, $q_0(x)$ is precisely the LP momentum and the interpolation formula for C for emission of gluon with transverse momentum q_t and fraction of energy x_j can be rewritten as follows:

$$C \;=\; \frac{1}{1 \;+\; \frac{x_0(q_t)}{x}\,\cdot\,\frac{q_0(x_j)}{q_t}}\,. \tag{39}$$

4.5 Correlations.

We assumed that there are no correlations between gluons in the cascade except for the fact that they are distributed in the disc of radius R. Then the probability to find two partons with the same value of $\ln\frac{1}{x_B}$ and $\ln Q^2$ (P_2) is

$$P_2 \;\propto\; \rho^2\,. \tag{40}$$

However this assumption is only correct in the case of a large number of colors ($N_c \to \infty$) [72]. If N_c is not large refs. [72] claim

$$\frac{P_2}{\rho^2} \to \exp\left(\sqrt{\frac{4N_c\alpha_s}{\pi}\ln\frac{1}{x_B}\ln\frac{Q^2}{Q_0^2}}\,\frac{1}{(N_c^2-1)^2}\right). \tag{41}$$

We would like to note that Bartels and Ryskin [37] found that such a correlation leads to a decrease of the correlation radius R by a factor of 1.3 - 1.4 in the HERA kinematic region.

It is also very instructive to write down the evolution equation that takes into account the correlation of eq.(41). We should mention that next-to-leading twist contributions were first related to what we defined as P_2 in [38]. It is a system of two equations, instead of the single equation of eq.(30),namely

$$\frac{\partial^2\rho}{\partial\ln\frac{1}{x_B}\partial\ln Q^2} = \frac{\alpha_s N_c}{\pi}\rho - \frac{\alpha_s^2\gamma}{Q^2}P_2\,, \tag{42}$$

$$\frac{\partial^2 P_2}{\partial\ln\frac{1}{x_B}\partial\ln Q^2} = \frac{4\alpha_s N_c}{\pi}\left(1+\frac{1}{(N_c^2-1)}\right)P_2 - \frac{2\alpha_s^2\gamma}{Q^2}P_2\rho\,. \tag{43}$$

Here we assumed that the probability to find three partons in the same cell of the parton phase space is $P_3 = P_2\cdot\rho$. Without this assumption the last term in eq. (43) reads as $2\alpha_s^2\gamma/Q^2\cdot P_3$. The general equation for P_n is (see ref.[46] for details)

$$\frac{\partial^2 P_n}{\partial\ln\frac{1}{x_B}\partial\ln Q^2} = \omega\gamma_n P_n - \frac{n\alpha_s^2\gamma}{Q^2}P_{n+1} \tag{44}$$

This equation indicates the need for the solution of two theoretical problems.

(i) We should find a general equation for γ_n, which has the formal meaning of the anomalous dimension of a high ($2n$) operator (refs.[46],[71], [72]).

(ii) We need a closed form of the equation which incorporates all P_n for the deep-inelastic structure function, and its solution.

The first problem was solved by A.G. Shuvaev and us in ref.[71]. The complicated problem of gluon-gluon interaction was reduced to that of interaction of colorless "gluon ladders" (Pomerons). It was shown in ref.[72] that this idea works for the case of the anomalous dimension of the twist four operator, in other words, for the case of P_2. The fact that we can consider the rescattering of n Pomerons to find γ_n (or P_n) signifies that we are dealing with a quantummechanical problem: the calculation of the ground state energy for an n-particle bosonic system where the interaction is attractive and given by a four-Pomeron contact term, with a coupling proportional to $\lambda = 4\alpha_s/(N_c^2-1)$. This observation simplifies the problem and enabled us te reduce it to solving the nonlinear

Schrödinger equation for n Pomerons in the t-channel. It should be stressed that this effective theory is a two-dimensional one, the two dimensions being spanned by $\ln\frac{1}{x_B}$ and $\ln Q^2$: the Schrödinger equation can be written for n particles on a line. It is well-known that this problem can be solved exactly (e.g. by Bethe Ansatz) and the answer was found to be

$$\gamma_n = \frac{N_c\alpha_s n^2}{\omega\pi}[1 + \frac{1}{3}\frac{1}{(N_c^2-1)^2}(n^2-1)] \tag{45}$$

Although Pomerons are bosonic, maximally two Pomerons occupy a single-particle level in this groundstate configuration, thus behaving like fermions. This is due to the two-dimensional nature of this problem. The second problem has also been (partly) solved by us (unpublished but see ref.[46] for results). We introduce the generating function

$$P(x_B, Q^2, \eta) = \sum_{n=1}^{\infty} P_n e^{n\eta} \tag{46}$$

with $P_1 = \rho$. Using eq.(44) we obtain

$$\begin{aligned}\frac{\partial^2 P}{\partial \ln\frac{1}{x_B}\partial \ln Q^2} &= \frac{N_c\alpha_s}{\pi}(P_{\eta\eta} + \frac{1}{3}\frac{1}{(N_c^2-1)^2}(P_{\eta\eta\eta\eta} - P_{\eta\eta}) \\ &\quad -\alpha_s^2\gamma e^{-\ln(Q^2)}e^{-\eta}(P_\eta - P),\end{aligned} \tag{47}$$

where $P_\eta = \partial P/\partial\eta$, $P_{\eta\eta} = \partial^2 P/\partial\eta^2$ etc. The deep-inelastic structure function is the solution of this equation at $\eta = -\ln(Q^2)$, viz.

$$x_B\, G(x_B, Q^2) = \pi R^2 P(x_B, Q^2, \eta = -\ln(Q^2). \tag{48}$$

Eq. (47) is a new evolution equation which allows one to take into account both initial and dynamical correlations between gluons in the parton cascade. The key problem in solving it is nonperturbative in nature, namely to determine an initial condition at $x_B = x_B^0$. The dependence of $P(x_B^0, Q^2, \eta)$ on η describes the correlations between gluons in the hadron near $x_B \sim 1$. The simplest case is to neglect this initial correlation and use the eikonal approach for $P(x_B^0, Q^2, \eta)$, namely

$$P(x_B^0, Q^2, \eta) = \sum_{n=1}^{\infty} e^{n\eta}\frac{(-1)^{n+1}}{n!}P_1(x_B^0, Q^2)^n = 1 - \exp(-e^\eta P_1(x_B^0, Q^2)) \tag{49}$$

The solution of this equation has not yet been found (see ref.[46] for more details).

5 A look at the first small x_B HERA data.

5.1 25 nb^{-1} experimental data.

Let us list conclusions from the first experimental results at small x_B from both collaborations at HERA (refs.[20]):

1. The increase of the value of the deep inelastic structure function F_2 at $x_B \to 10^{-4}$ shows that the gluon density reaches sufficiently big value,namely

$$x_B G(x_B, Q^2) \to 40 - 50 \text{ at } x_B = 10^{-4} \text{ and } Q^2 = 20 GeV^2 .$$

The value for $x_B G(x_B, Q^2) = 50$ was determined from the $MRSD-'$ parametrization that roughly describes the new data.

2. The ZEUS collaboration measured the diffraction dissociation[5] cross section and found

$$\frac{\sigma^{DD}}{\sigma_t} = \frac{5.2nb}{80nb} = 6\,10^{-2} \text{ at } x_B = 10^{-4} \text{ and } Q^2 > 10 GeV^2 .$$

We will say more about this shortly.

3. F_2 experimental data can be described by the GLAP evolution equation assuming that at the initial vituality $Q_0^2 \sim 5GeV^2$ the gluon structure function rapidly increases at $x_B \to 0$ as $x_B G(x_B, Q_0^2) \propto x_B^{-\omega_0}$ and $\omega_0 \geq 0.3$.

4. Both collaborations measured the total photoproduction cross section both for very small virtualities of the incoming photon and for real photons. This cross section exhibits a common property of "soft" processes, namely $\sigma_t \to s^{-\Delta}$ where $\Delta \sim 0.08$.

5.2 The value of SC from HERA data.

Let us first try to see how the large number of gluons (40-50) can be understood. We believe that an interesting way to do this is to compare the proton at $x_B = 10^{-4}$ and $Q^2 = 15GeV^2$ with an iron nucleus, which has a similar amount of nucleon constituents. Calculating the packing factor by assuming the size of the constituents to $R_N = 0.86Fm$ for the nucleons, and $R_G^2 = 1/Q^2$ for the gluons, we find that if one assumes the size of the gluon disc to be $R_N/3$ (section 4.2), that the two packing factors are very similar. Thus, in this sense, we see that a proton $x_B = 10^{-4}$ and $Q^2 = 15GeV^2$ is very similar to an iron nucleus.

[5] Diffraction dissociation is the process in which a number of hadron is produced, and one recoiled proton, whose fraction of energy is close to one.

We now estimate the size of shadowing corrections for the deep-inelastic structure function. Let us write it as

$$F_2(x_B, Q^2) \;=\; F_2^{GLAP}(x_B, Q^2) \;-\; \Delta F_2(x_B, Q^2)\;, \tag{50}$$

where F_2^{GLAP} is the solution of the usual (GLAP) evolution equation and ΔF_2 is the SC. A straigtforward estimate gives

$$\frac{\Delta F_2}{F_2} \;\propto\; \alpha_s < r_G^2 > \rho \;\to\; 0.1 \text{ for } Q^2 = 15\,GeV^2 \text{ and } x_B = 10^{-4}\;. \tag{51}$$

However the ZEUS data on diffraction dissociation let us estimate the value of SC better. Indeed, it was shown in ref. [36] that we have the following relationship between SC and the DD cross section

$$|\Delta F_2| \;=\; F_2^{DD}\;, \tag{52}$$

where F_2^{DD} was defined in ref. [36]. In other words $|\Delta\sigma_t/\sigma_t| \;=\; \sigma^{DD}_{\gamma^* p}/\sigma_t$. where σ_t is the total photoproduction cross section. From the ZEUS data we can then conclude: $|\Delta F_2|/F_2 \;>\; 6\cdot 10^{-2}$. Note that in this case we can not just begin to discuss the question whether there is SC, but even whether we could predict this SC value in our theory.

We remark that the details of the evolution equation for F_2^{DD} were discussed in ref.[36], where it was suggested to measure the sum $F_2 + F_2^{DD}$ in which all contributions of SC are cancelled. Thus for this sum one can use the GLAP equation even at small x_B.

5.3 Saturation of the parton density or different physics for "soft" and "hard" processes?

The HERA data allow us to raise the question which we put in the title of this subsection. Indeed, we can distinguish two regions in Q^2 that have quite different energy behavior of the photoproduction cross section and will list the experimental facts that pertain to these regions.

1. $Q^2 \;\ll\; 1\,GeV^2$. (i) The total cross section is essentially constant here (or increases slightly with energy); (ii) $\frac{\sigma^{DD}}{\sigma_t} \;\approx\; 10\%$. Thus in this kinematic region the photoproduction process with small values of photon virtualities seems to be typical soft process like a hadron-hadron collision.

2. $Q^2 \;>\; 5\,GeV^2$. (i) The total cross section increases rapidly with energy (x_B) $\sigma_t \;\propto\; x_B^{-\omega_0}$; (ii) $\frac{\sigma^{DD}}{\sigma_t} \;\sim\; 10\%$. This is the typical deeply inelastic scattering process. Both experimental facts can be interpreted as arising from the contribution of a so-called "hard" Pomeron, which is a solution to the BFKL

equation [21] and leads to $\sigma_t \propto x_B^{-\omega_0}$ with $\omega_0 > 0.4$ while the smallness of the ratio $\frac{\sigma^{DD}}{\sigma_t}$ has a natural explanation in the small values of SC.

The question arises what happens for intermediate value of photon virtualities $1GeV^2 < Q^2 < 5GeV^2$. Two different scenarios for this kinematic region exist:

Landshoff picture: At $Q^2 < 1GeV^2$ all experimental data for photoproduction as well as for other soft processes can be described by exchange the soft Pomeron which is the old Regge pole with intercept $\alpha_P = 1 + \epsilon$ ($\epsilon \sim 0.08 \ll \omega_0$) (see ref.[39]). The small value of the ratio $\frac{\sigma^{DD}}{\sigma_t}$ can then be interpreted as an indication that the SC are small and can be treated in a perturbative way in this approach. In particular Donnachie and Landshoff considered only two Pomeron exchange. In this picture the region of deeply inelastic scattering has different underlying physics, rather related to a hard Pomeron. The transition between the "hard" and "soft" regions seems quite arbitrary at the moment. However this approach is very simple and provides an elegant description of all available experimental data on "soft" processes.

Saturation of the parton density: The second scenario is intimately related to the hypothesis of parton density saturation. In this scenario the "hard" Pomeron is responsible for the behavior of the total gross section in both kinematic regions, but the small value of the ratio $\frac{\sigma^{DD}}{\sigma_t}$ is interpreted differently for large and small virtualities: for large virtualities it supports a small value of SC, while at small ones we interpret it as an indication that the SC becomes very large and leads to the black constituent quark disc. The greatest advantage of this scenario is the unified description of both the diffractive and inclusive process, and that it is based on solid theoretical background, namely properties of the "hard" Pomeron and the shadowing correction in perturbative QCD. However we have to note that a description of the data has not yet been done within this hypothesis, in spite of the fact that these two scenarios lead to sufficiently different behavior in the region of intermediate virtualities of photon. In the second scenario we expect some transition region with smooth behavior of σ_t versus Q^2. A first try to extract this behavior from available experimental data shows that such a transition region does not contradict them [47] but it is still too early to draw a definite conclusion from the data.

6 Predictions.

6.1 The structure of the typical inelastic event.

Here we are going to discuss how the new phenomena will manifest themselves at high energies. As discussed the most important prediction that originated

from QCD is the appearance of a new scale $q_0(x)$ for the transverse momentum of the partons. For phenomelogical purposes we make here the following ansatz for $q_0^2(x)$ [63]:

$$q_0^2(x) \;=\; \mathbf{Q_0^2} \;+\; \mathbf{\Lambda^2} \cdot exp(3.56\sqrt{\ln \frac{\mathbf{x_0}}{x}}) \;, \tag{53}$$

where we introduced three phenomenological parameters $(\mathbf{Q_0}, \mathbf{\Lambda}, \mathbf{x_0})$ to describe the low energy behavior of $q_0(x)$. These parameters cannot be calculated in perturbative QCD and we have only estimates from QCD sum rules. There are some attempts to extract the values for these parameters directly from inclusive jet production using formulas (18). One finds that $\mathbf{Q_0} = 1.4$ GeV, $\mathbf{\Lambda} = 52$ MeV and $\mathbf{x_0} = 1/3$ ([40]). With these numbers one can estimate typical values of $q_0(x)$ for various colliders. E.g. for the Tevatron at a value of $x = 1.8 \cdot 10^{-3}$ one has $q_0(x) = 3.3GeV$. This is a typical value and thus the transverse momentum much larger than the observable transverse momentum of a produced hadron ($\approx$ several MeV). However these two transverse momenta are compatible if one takes into account the fragmentation of partons into hadrons [40].

Thus we can formulate the first prediction:

The main source of secondary hadrons is provided by semihard processes in which the gluon (quark) jets are created with transverse momentum $k_t \sim q_0(x)$, decaying eventually into hadrons.

In other words, in QCD the inclusive production of hadrons which seems to be a typical "soft" process instead is "hard" and thus calculable in perturbative QCD. The most straightforward consequences of the semihard origin of multiparticle production are

1. a significant growth of the transverse momentum for the hadron minijets: $q_t \propto q_0 \sim \Lambda exp\,(\,1.25\,\sqrt{\ln s}\,)$;

2. a rapid increase of the total multiplicity: $N \propto q_0^2 \sim exp\,(2.52\,\sqrt{\ln s}\,)$;

3. a decorrelation effect for jets with transverse momentum k_t of the order of q_0. The value of transverse momentum for such a jet is compensated not by one jet in the opposite direction but by a number of jets with average transverse momentum about q_0.

The above essential ideas about semihard processes lie at the basis of all available Monte Carlo programs for simulation of typical inelastic events at high energies.

6.2 Total cross section in QCD.

The total cross section of deeply inelastic scattering is directly related to the parton density (see eq.(15)). However the previous discussion shows that we

need more theory in the region of *high density QCD* in order to understand the behavior of the total cross section, especially if we are going to discuss the cross section of hadron - hadron interaction beyond merely the deeply inelastic case. To learn the main properties of this total cross section we have to understand better the parton distribution in impact parameter (b_t) space. It is well known that each parton takes part in a random walk in b_t (ref.[49]). This random walk provides a unique mechanism for an increase of the interaction radius at high energy. This follows directly from the uncertainty principle:

$$\Delta b_t q_t \approx 1 \ \ or \ \ \Delta b_t \approx \frac{1}{q_t}\,, \tag{54}$$

where Δb_t is the change of the impact parameter of the parton for a single emission in the parton cascade while q_t is the typical transverse momentum for such an emission. In section **4.4** we have shown that $q_t \to q_0(x)$ at high energy; since $q_0(x)$ is big the displacement Δb_t for each parton decay (emission) becomes negligibly small. In other words the appearance of a new scale in the parton cascade leads to all partons being frozen in b_t. Thus sooner or later the parton density at fixed b_t reaches its limiting value at sufficiently high energy within the framework of **parton density saturation** hypothesis.

Let us assume that all partons at $b_t < R(s)$ have reached the saturation value of parton density and then try to understand what happens when a new parton is emitted. If the emission takes place inside of the disc of radius $R(s)$ ($b_t < R(s)$) the emission cannot change anything since the new parton will be absorbed by nearby partons just after its production. However if the new parton is emitted just on the edge of the parton disc ($b_t \approx R(s)$) it can go outside of the disc, its displacement in b_t depending on the minimal transverse momentum in such a decay (emission) Q_0. Again, the parton cannot go into the disc due to the strong absorption there. Thus, the change of the radius is

$$\frac{dR(s)}{dlns} \propto \frac{\omega_0}{Q_0}\,,$$

where ω_0 is the probability of gluon (parton) emission (see section **2.2**) and Q_0 is the minimal transverse momentum. Q_0 is the purely phenomenological parameter that we would like to keep equal to Q_0 in eq.(53) because these two values have the same physical meaning. Even these simple arguments show that we need some additional assumptions to deal with the problem of the total cross section.

However the main property of the behavior of the total cross section as well as the diffractive dissociation cross sections follow directly from the hypothesis

of parton density saturation. Our second prediction can then be formulated as follows:

A fast hadron interacts with the target as a black disk with a radius that increases with energy as $R(s) = \frac{\omega_0}{Q_0} \ln s$.

The value of energy and the preasymptotic behavior depend very strongly on other phenomenological assumptions.

Summarizing this subsection we emphasize that in spite of the fact that the total cross section as well as other exclusive processes at high energy need a nonperturbative approach, the general property of the parton cascade in QCD together with only one phenomenological assuption (*parton density saturation* hypothesis) allows us to predict a principal feature of their high energy behavior. We hope that this prediction can play a guiding role in such a future nonperturbative approach to the problem.

6.3 The Mueller - Navelet processes ("hot spot" hunting).

The brief discussion in the previous section has made clear that we cannot rely only on the main properties of a typical inelastic event if we want to see a indications of new physics. The theory gives us quite transparent predictions for a typical event but we have not yet found a theoretically selfconsistent way to estimate the value of energy at which all new phenomena enter into the game. So we must invent experiments such that new physics manifests itself most directly.

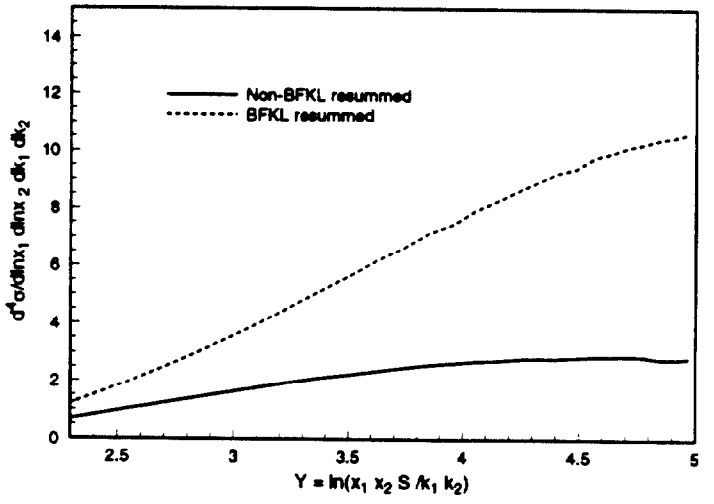

Figure 10: Differential cross section for two-jet production vs. rapidity difference of the two jets. Here x_1, x_2 are the momentum fractions of the jets, and the k_i $(i = 1, 2)$ are their transverse momenta.

One way to penetrate the interesting kinematic region is via so-called Mueller-Navelet processes [50]. The main idea of this approach is to create an experimental situation in which we can measure the parton density in a small region ("hot spot") inside a hadron. Since the distances in such processes are small we can predict better the increase of parton density as well as the value of shadowing corrections which are sizable here (R^2 in the master equation (30) is small).

The simplest Mueller - Navelet process is inclusive single jet (x_j, k_t) production in deeply inelastic scattering in the kinematic region where $x_B \ll x_j$; $k_t^2 \approx Q^2$. In such a process the virtual photon probes the region of a proton that is small ($r_{hot\,spot} \propto \frac{1}{k_t} \ll R_{proton}$). At a sufficiently small value of the ratio $\frac{x_B}{x_j}$ one penetrates directly the region of *high density QCD* in Fig.4 where we anticipate a significant increase of parton density and large SC. HERA is planning to measure this process and it has been discussed in many papers (see ref.[51] for detailed information on this subject for experts).

In hadron - hadron collisions we can create a similar situation if we measure the double inclusive cross section of two-jet production with large but equal transverse mopmenta $k_{1t} \approx k_{2t}$ and sufficiently large rapidity difference between them. Fig.10 shows our preliminary estimates for this Mueller - Navelet process at Tevatron enegies. See also [52]. One can see that the cross section of such a process is not small and that the difference between standard approach based on the GLAP evolution equation and the new one that implemented the new physics of section **2** is also seems sizable. Thus we can say

For Mueller - Navelet processes we expect strong energy dependence $\sigma \propto s^{\omega(k_t)}$ *if all* x *for jet or virtual photon are fixed, plus a sizable shadowing effect.*

6.4 Diffraction Dissociation (DD).

We introduced diffraction dissociation in the section **5** and hopefully convinced the reader that this process yields direct information on the size of the shadowing correction. We emphasize that in this process one measures the structure function of the Pomeron in first approximation [53]. In spite of the fact that we have not understood what a Pomeron is, it is clear that it is small ($r_{Pomeron} \approx 0.2Fm \ll R_{proton}$). Thus DD in deeply inelastic scattering is one more way to measure the parton density for a gluon system confined in a small volume.

The modification of DD in DIS for hadron - hadron colliders is so called "hard" diffraction, namely the production of two jets with large transverse

momenta in DD process [54] for example $p + p \to jet(k_{1t}) + jet(k_{2t} \approx k_{1t}) + X + p(x_F \to 1)$. At the moment not all properties of this process are clear, some refs. are [53] [54] [55]. Nevertheless we are able to claim:

Diffractive dissociation processes give us a measurement a parton system confined in a small volume which can be treated theoretically in a selfconsistent way.

6.5 Large Rapidity Gap (LRG) processes.

Bjorken has suggested a new class of processes [56] that would allow us to enter the high density QCD region and check experimentally ideas on the Pomeron structure, shadowing corrections and the gluon density in a hadron. These are the processes with a large rapidity gap [6].

To understand what is interesting about these processes let us consider a particular one: two gluon-jet production with rapidities y_1 (y_2) and transverse momenta k_{1t} (k_{2t}) respectively. The signature for LRG process is :

1. $\Delta y = |y_1 - y_2| \gg \langle y \rangle$, where $\langle y \rangle$ is the mean rapidity difference between two jets with the same value of transverse momenta ; 2. $|\mathbf{k_{1t}} + \mathbf{k_{2t}}| = |k_{out}| \leq \langle q \rangle_t$,where $\langle q \rangle_t$ is the mean transverse parton momentum in the parton cascade; 3. no particles are produced with rapidities between y_1 and y_2.

The cross section of the above process can be written in a form that is a straightforward generalization of eq.(18):

$$\frac{d\sigma(A + B \to jet(y_1, k_{1t}) + jet(y_2, k_{2t}) + X + (LRG\, y_1 - y_2))}{d\Delta y dk_{1t}} =$$

$$S(y_1, y_2) \sum_{ab} \int dx_a dx_b d^2k_{at} d^2k_{bt} d^2k_{out}\, \Phi_{a/A}(x_a, k_{at})\, \Phi_{b/B}(x_b, k_{2t})$$

$$\mathcal{I}(x_a x_b s, k_{at}, k_{bt}, k_{1t}, k_{2t}) \delta^{(2)}(\mathbf{k_{at}} + \mathbf{k_{bt}} - \mathbf{k_{out}}) \,. \quad (55)$$

We now expand on three main features of this equation

1. The factor $S(y_1, y_2)$ is the so-called survival probability of the LRG. The physical meaning of it is very simple in the parton (QCD) language: it is the probability that there is no inelastic interaction between partons with $x > x_a$ from hadron A and partons with $x > x_b$ from hadron B. Unfortunately, we need a much better understanding of so-called "soft" processes to calculate $S(y_1, y_2)$. However simple estimates in the eikonal model [56][58] show that $S \approx 5 - 20\%$. Therefore LRG processes can be measured experimentally. Let us however issue

[6] We note that the first LRG process was considered by Dokshitzer, Khoze and Sjostrand [57]. Bjorken generalized the approach and formulated it as a new tool to study "semihard" physics.

several warnings: i) in an eikonal approach S does not depend on y_1 and y_2 and is merely a function of the collision energy. This is not correct in a more general approach. For example in deeply inelastic scattering where we know more about the structure of the parton cascade S turns out to be a complicated function of all variables: s, y_1 and y_2 [59]; ii) the source of a LRG can be also the usual statistical fluctuation in a system of produced partons as well as produced hadrons in typical inelastic events without LRG. Such fluctuations lead to $S \propto e^{-\kappa\Delta y}$ where the value of κ is strongly correlated with the model used for a typical inelastic event in a high energy hadron - hadron collision. Some attempts have been made to calculate κ at the partonic level [60] but the only way to calculate this coefficient for the hadronization is to use a Monte Carlo model. In general $\kappa \propto \rho$ so for the parton cascade with a large density of partons κ could be large enough to effectively suppress this possibility.

2. The flavors a and b for jet production are predominantly gluons so this process gives us an unique possibility to measure directly the gluon density. Recall that in deeply inelastic processes for example we measure mainly the quark density since the photon interacts with a quark. Since the cross section for LRG jet production depends mostly on the square of the gluon density the LRG process can be a good tool to measure this density.

3. The impact factor $\mathcal{I}$ in the above formula is the most interesting object since the main contribution to it at high energy ($x_a x_b s \to \infty$) is the exchange of a "hard" Pomeron.

$$\mathcal{I} \to \frac{1}{k_t^2}[x_a x_b s]^{\frac{\alpha_s(k_t^2)N_c}{\pi}\cdot 4\ln 2}$$

The proof of this statement can be found in [61] while the expression itself was first written in ref.[54]. The problem in the present understanding of the LRG processes is the fact that we do not know how large the energy for which this simple formula is valid should be. As was pointed out by Bjorken [56] the impact factor in Born approximation (two gluon exchange) gives an answer which is proportional to

$$\frac{1}{k_t^2}\int_{\frac{1}{R^2_{hadron}}}^{k_t^2}\frac{dl^2}{l^2}\,.$$

Therefore in Born approximation our Pomeron consists of one gluon with a virtuality of the order of large k_t^2 (i.e. its size is small, $r_{G_1} \propto \frac{1}{k_t}$) while the second gluon has a small virtuality (l^2) and $r^2_{G_2} \propto \frac{R_{hadron}}{k_t}$. Thus the Pomeron is quite a large object in Born Approximation and cannot be considered a point like probe, as was assumed in eq.(55).

We would like to conclude that in spite of many yet unsolved theoretical problems, a LRG trigger can yield new insight into the Pomeron structure in the region where it is governed by perturbative QCD. We can summarize the main properties of LRG processes by:

LRG processes are new probes of gluon densities at high energy and the Pomeron structure. The cross section of LRG processes should decrease exponentially for sufficiently small Δy, reach some plateau at intermediate Δy and rise exponentially at large values of Δy ($\propto exp(\omega_0(k_t)\Delta y) \sim exp(\frac{\alpha_s(k_t^2)N_c}{\pi} \cdot 4\ln 2 \cdot \Delta y)$).

The first D0 measurement [62] encourages further detailed and careful experimental study of such processes.

6.6 Interaction with a nucleus.

Here we investigate what the microscopic theory of QCD can tell us about interactions with a nucleus. In this subsection we try to answer two questions:

- Why is a nucleus a better target for probing the high-density QCD region than a hadron?
- How do the new phenomena in the high parton density region manifest themselves in ion-ion collisions?

6.6.1 Why is a nucleus a better target?

The short answer to this question is: perturbative QCD works better for the case of a nucleus. This can be argued as follows.

First, the density of partons in the parton cascade of a fast nucleus is much larger than for a hadron because each nucleon is able to produce its own chain of partons. Consequently, in the case of a nuclear target one can reach the *high density QCD* region at smaller (reasonable) values of the energy. As we have discussed before we can apply perturbative QCD here since the typical partobn transverse momentum is sufficiently large.

Secondly, the typical transverse momentum for partons is larger for the case of a nucleus than for the hadronic case. To clarify this statement let us consider the unitarity constraint for the parton density in a nucleus (see section **2.3**). Unitarity tells us that

$$\sigma(\gamma^* A) \ll \pi R_A^2. \tag{56}$$

For a nucleus $R_A \propto R_{proton} A^{\frac{1}{3}}$ and in first approximation (when the cross section $\sigma(\gamma*, N)$ is small) $\sigma(\gamma^*, A) = A\sigma(\gamma^*, N)$. Thus we can rewrite the

unitarity constraint of eq. (56) using the notation of eq. (26) as follows:

$$W_N \leq A^{-\frac{1}{3}} \tag{57}$$

while for a nucleon $W_N \leq 1$.

Fig.11 shows that eq. (57) leads to an increase of the typical transverse momentum in nucleus parton cascade in comparison with the nucleon case ($q^2_{0,A} \gg q^2_{0,N}$).

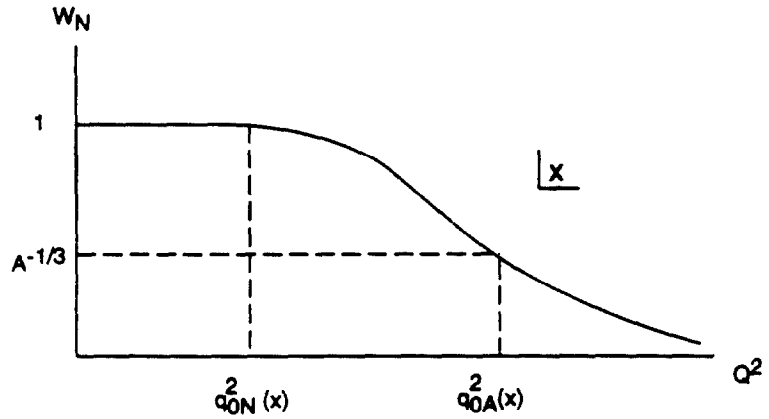

Figure 11: The dependance of W_N on Q^2 at fixed x.

As has been discussed in section **4.4**, the typical parton momentum $q_{0,A}$ plays two roles in a collision process: i) $\frac{1}{q_{0,A}}$ is the maximal size of the constituents (partons) that can be differentiated in the parton cascade; ii) $q_{0,A}$ is the Landau - Pomeranchuk momentum for the parton system after the first collision, where the coherence was destroyed. It means that due to the Landau-Pomeranchuk effect a parton with a smaller value of the transverse momentum cannot be produced. Finally we are able to conclude that the typical distances R in any nucleus reaction is smaller than $\frac{1}{q_{0,A}}$ ($R \ll \frac{1}{q_{0,A}} \ll \frac{1}{q_{0,N}}$). In other words the typical value of the QCD coupling constant (α_s) for the case of the nucleus should be smaller than for hadron reactions (see ref.[40] for a more detailed discussion on this subject).

In short:

Typical distances in the interaction with a nucleus are smaller than in interaction with a hadron, so that pQCD series should converge faster for the nuclear case than for the hadronic case.

6.6.2 How do the new phenomena anticipated in high density QCD manifest themselves in interactions with a nucleus?

The basis of our approach is the nonlinear GLR equation for parton recombination in the parton cascade (section **4.1**). In the case of a nucleus we can follow the same reasoning as in section **4.1** and obtain the equation for the gluon density in a nucleus. It has the form [63]:

$$\frac{\partial^2 x G_A(x,Q^2)}{\partial \ln \frac{1}{x} \partial \ln Q^2} = \frac{\alpha_s N_c}{\pi} x G_A(x,Q^2) - \alpha_s^2 \frac{9N_c^2}{2(N_c^2-1)R^2}[x G_A(x,Q^2)]^2 - \frac{9N_c^2}{2(N_c^2-1)} T [x G_A(x,Q^2)]^2 , \quad (58)$$

where the first two terms describe the parton recombination in one nucleon while the third term diminishes the gluon density due to interaction between gluons from different nucleons in a nucleus. The coefficient T in eq. (58) is different in three different kinematic regions and it is equal to:

$$T = 4\pi T(b_t) = 8\pi\rho\sqrt{R_A^2 - b_t^2} \text{ for } x < x_b \text{ or } \tau > \sqrt{R_A^2 - b_t^2}$$
$$T = 4\pi T(b_t)\frac{x_b}{x} \text{ for } x_0 > x > x_b \text{ or } R_{proton} < \tau < \sqrt{R_A^2 - b_t^2}$$
$$T = 0 \text{ for } x > x_0 \text{ or } \tau < R_{proton} , \quad (59)$$

where $\tau = 1/mx$ is the life time of the virtual probe of the gluon density, $x_b = \frac{1}{2m\sqrt{R_A^2 - b_t^2}}$ is the value of x for which the probe lives just long enough to cross the nucleus at impact parameter b_t, whereas x_0 is defined by $1/mx_0 = R_{proton}$, m being the proton mass. The three regions correspond to the situation when the probe interacts with all nucleons in a nucleus, with a smaller number of nucleons ($\rho\tau < T(b_t)$) and with the parton inside one nucleon, respectively.

A remarkable property of this equation is the fact that the third term has no ambiguity (unlike the second terms which depends on the parameter R^2) and all coefficients are well defined. The numerical solution of eq.(58) has been studied in ref. [64] where it has been shown that the solution to eq. (58) is able to describe the available experimental data. Thus this equation gives us a reliable basis for estimates of the influence of the parton recombination on different observables in hadron-ion and ion-ion collisions. As we have discussed in section **3** two approaches can be developed to multiparticle production in nuclear collisions:

i) the first one is based on the factorization theorem. Its starting point is the expression for inclusive production (see eq.(7)) with which we are able

to calculate the inclusive cross section if we know the parton density. In this approach the master equation (58) provides the theoretical basis to perform such calculations. The calculated value of inclusive density of produced partons can be used to develop a Monte Carlo program to simulate a typical inelastic event.

ii) the starting point of the second approach is the transport equation from section **3.4** for the spatial density of partons $F(\mathbf{p}, \mathbf{r}, t)$ in real time. Here the kernel of the problem lies in the collision integral I and in the method of taking into account coherence effects in a medium.

The master equation (58) and the hypothesis of parton density saturation yield a new strategy, namely to introduce the new scale of momentum $q_{0,A}$ with the aim of treating processes with transverse momenta larger than $q_{0,A}$ in perturbative QCD while treating processes with smaller transverse momenta with the parton density saturation assumption, and introducing the value of the maximal parton density ($\Phi_{0,A}$) as a phenomenological parameter.

This strategy has been realized only partly the various Monte - Carlo programs for ion - ion and hadron - ion collisions that are on the market (see refs. [33] [34][65]). All of them are based on the *semi - hard* approach which has been discussed in the above. They use the appearance of a new sufficiently large scale (q_0) for the transverse momentum of partons and apply perturbative QCD to describe the major part of the total inclusive cross section. However none of them treat correctly the energy and A dependence of this new typical transverse momentum and the appearance of the limiting value of the gluon density.

However these attempts are very instructive since they give the first numerical estimates for the probability of creating especially in ion-ion collisions a new aggregate phase of hadronic matter, the *quark-gluon plasma* at high energy. The result of these calculations can be summarized by the statement that at RHIC or LHC energies we expect that an ion-ion collision proceeds in two stages: equilibrium of gluons after $\tau_G \approx 1/2Fm/c$ and production and equilibrium of quarks after a longer time $\tau_q \approx 2Fm/c$ [66]. We think that the values of these characteristic times are rather premature since the number of collisions has been overestimated in available calculations because the Landau-Pomeranchuk effect and the existence of the limiting parton density (both diminish number of produced partons) have not been taken into account properly. However the appearance of two stages in these processes as well as the large number of collisions arise very naturally in the semi-hard approach and we hope that we made this fact plausible. The second important lesson from these exercises is the fact that perturbative QCD is responsible for the preequilibrium stage so it means that sooner or later we be in a position to describe ion -ion collisions theoretically.

In short:

The semi-hard approach or what we know theoretically about high density QCD allows us to develop a theoretical approach to ion-ion and ion-hadron collisions in which two stages appear naturally: gluon equilibrium after a short time and quark equilibrium after a much longer time.

6.6.3 The factorization theorem in nuclear scattering.

We would like to finish this short section on nucleus collisions by discussing the factorization theorem for nuclear collisions. Our statement is based on the physical meaning of $q_{0,A}(x)$ as the Landau-Pomeranchuk momentum for a nucleus. Recall that the rescattering of partons inside the medium leads to a suppression of emission if the transverse momentum of the emitted parton, p_t, is smaller than the Landau-Pomeranchuk momentum ($p_t < q_{0,A}(x_B)$). Therefore for inclusive production of a jet with $p_t >> q_{0,A}(x_B)$ one can use the usual factorization theorem and express the inclusive cross section through the product of parton densities. However when $p_{t\,\rm jet} < q_{0,A}(x_B)$ the factorization theorem is no longer applicable. For transverse momenta that small we cannot use the language of the parton densities to calculate the inclusive cross section. Formally, this means that when $p_{t\,\rm jet} \simeq q_{0,A}(x_B)$ higher twist contributions become essential and thus the formal proof of the factorization theorem in [17] no longer applies. For such small transverse momenta we cannot use the language of the proton densities to calculate the inclusive cross section. In the region where $p_{t\,\rm jet}$ is not too much larger than $q_{0,A}(x_B)$ we can use the transverse momentum factorization approach, using parton densities, and taking into account screening corrections using the GLR equation. A more detailed discussion of this problem is beyond the scope of this review, but we would like to draw attention to this problem, which is often misunderstood, leading to either neglecting the LP effect for all $p_{t\,\rm jet}$, or using the LP approach even for very large values $p_{t\,\rm jet}$ (e.g. [75]).

7 Conclusions.

We can perhaps summarize the above by the following statements.

- The new kinematic region of *high density QCD* is still wide open for theoretical and experimental investigation.
- Perturbative QCD methods have been developed to explore the transition region between the region routinely analyzed by perturbative calculations for "hard" processes and the high density QCD one.

• It was shown that between the kinematic region of "soft" processes (key words: unitarity, analyticity, reggeons, Reggeon Calculus, hadronization models ...) and the kinematical region of "hard" processes (key words: quarks, gluons, parton distributions, asymptotic freedom, pQCD, evolution equations ...) there is the region of **semi -hard processes** where the cross sections can be so large as to be of the order of the geometrical size of the hadron but with a typical transverse momentum large enough that methods of perturbative QCD can be applied.

• New probes for this high density QCD region have been developed. In spite of the fact that we still lack some theoretical understanding and the ability to provide reliable estimates for such probes we firmly believe that these probes give a deeper insight into QCD and could lead to new experimental discoveries.

7.1 Phase transition.

We can represent the predictions of the previous section as a phase transition between different forms of hadronic (partonic) matter. Our prediction can then be summarized as the possibility of a phase transition from a *Quark - Gluon Ideal gas* to a *Gluon Liquid* (see Fig.11).

Indeed in the *pQCD* region (see Fig.5) we can regard a partonic system as an ideal gas of quarks and gluons since we can neglect their interactions (only emission being esssential here).

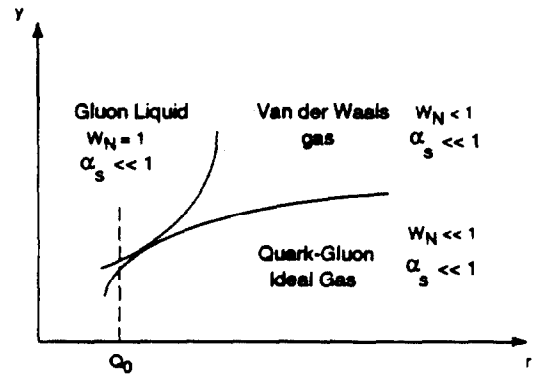

Figure 12. The phase diagram for hadron-hadron collisions for rapidity $\eta = 0$ in the cm frame. Here $y = \ln s$, $r = \ln p_t^2$ and W_N is defined in eq.(26).

When the density of partons increases we approach the region where we have to take into account the interactions between partons in a simple approximation

and in a situation where this interaction is not too big. This then is a Van der Waals gas of quarks and gluons. Here we have a theory based on a nonlinear evolution equation which plays the role of the Van der Waals equation for a parton system.

For even larger values of the density we have a situation where the density is large but the value of coupling constant is still small. This smallness leads to a small correlation between partons. This is the reason we call this system of partons a *Gluon Liquid*. We recall that the density is high mostly due to emission of gluons and quarks inside this system can still be treated in a perturbative way.

The borders between these different regions are the critical line we discussed in section **4.3** (between *GL* and *VdWG*) and the trajectory of the GLAP evolution equation that touches the critical line (between *VdWG* and *QGIG*). The asymptotics of these borders are also calculable.

7.2 Where we stand.

Let us summarize where we stand at the time of writing in the theoretical development of small x physics.

1.In pQCD we are struggling with two major problems: i) our perturbative series have a naturally small parameter α_s but its smallness is often compensated by large logarithms which are different in different processes. In the case of small x processes the real expansion parameter of the perturbation series is $\alpha_s \ln \frac{1}{x}$ which is not small. ii) the perturbative series is asymptotic since the coefficient C_n (see eq.(9) for example) behaves as $n!$ at large n.

The first problem is mainly technical and is solved by the BFKL equation [21]. However this equation suffers from two problems: the next order corrections have yet not been found while experience with calculating part of them shows that they are large [67]; also, this equation feels the as yet ununderstood confinement region. Moreover, such confinement corrections have not been localized in something like a matrix element of some operator and the only way how we are able to treat them is to introduce by hand some momentum cutoff. Remarkable progress has been made recently by Mueller [68] who gave a very transparent derivation of the BFKL equation and constructed the parton wave function for the parton cascade in the region of small x.

The second problem is very complicated and could be solved only if we understand better the nonperturbative origin (renormalons, instantons,...) of such a behavior of coefficient C_n. Unfortunately even for the simplest case of the total cros section in e^+e^- annihilation this has not yet been done (see ref.[69]). We should mention that a first attempt has been made to calculate

the instanton contribution to the deep-inelastic structure function [70].

2. Progress in the understanding of shadowing corrections is intimately related to resummation of the perturbation series in the new small parameter W. The GLR equation is the result of such resummation. A recent development was the understanding that such a resummation in terms of the Wilson Operator Product Expantion implies that we have to take into account the high twist contributions. They must be important because the anomalous dimension of high twist operator turns out to be very large at small x, so large in fact that it can compensate the extra power of $1/Q^2$ in the high twist contribution [71]. At the moment the anomalous dimension of twist four gluonic operator has been calculated [72] as well as the value of the anomalous dimensions of all higher twist operators within a specific approximation [71]. The corresponding generalization of the GLR equation has been discussed in section **4.5**.

3. The hope to develop a nonperturbative approach to the problem of small x is mostly connected with the attempt to write down an effective lagrangian for the region of small x. Implicitly one assumes that such a lagrangian should be simpler than the QCD one and should allow one to apply some numerical procedure (lattice calculation for example) to calculate scattering amplitudes with this lagrangian. It has so far been impossible to calculate actual amplitudes with the full QCD lagrangian. At the moment we have two effective theories on the market: one by Lipatov [73] which looks not much simpler that the full QCD one but incorporates all results of perturbative calculations, the second one is by Verlinde and Verlinde [74], and is much simpler and is also suited for lattice -like calculation but it has not yet been checked how well this effective theory describes perturbative results.

We hope that these issues clearly illustrate how far removed we still are from the goal of obtaining an analytical solution of the problem of small x physics. Moreover, we hope that our review demonstrates how interesting and difficult the problem is. We did our best to excite the interest of theoretical theorists, practical theorists and experimentalists alike in the beauty and charm of high density QCD.

Acknowledgements

E. Levin would like to thank the Fermilab theory for hospitality.

References

[1] M. Gell-Mann, *Phys. Lett.* **B8** : 214 (1964); G. Zweig, CERN-Report-8182/TH - 401 (1964); CERN-Report-8419/TH-412 (1964).

[2] O.W. Greenberg, *Phys. Rev. Lett.* **13** : 598 (1964).

[3] I.S. Hughes, *Elementary Particles* Cambridge: Cambridge University Press (1991).

[4] C.N. Yang, R.L. Mills, *Phys. Rev.* **96**: 191 (1954).

[5] H. Fritzsch, M. Gell-Mann, H. Leutwyler, *Phys. Lett.* **B47** : 365 (1973); D.J. Gross, F. Wilczek, *Phys. Rev.* **D8** : 3633 (1973); S. Weinberg, *Phys. Rev. Lett.* **31** : 494 (1973).

[6] CTEQ Collaboration. *Handbook of Perturbative QCD*, ed. G. Sterman. Fermilab preprint FERMILAB-PUB-93/094-T; G. Sterman, *An Introduction to Quantum Field Theory* Cambridge: Cambridge University Press (1993).

[7] D.J. Gross, F. Wilczek, *Phys. Rev. Lett.* **30** : 1343 (1973); H.D. Politzer, *Phys. Rev. Lett.* **30** : 1346 (1973); G. 't Hooft, *Phys. Lett.* **B61** : 455 (1973); *Phys. Lett.* **B62** : 444 (1973); I.B. Khriplovich, *Yad. Fiz.* **10** : 409 (1969).

[8] L.D. Landau, A.A. Abrikosov, I.M. Khalatnikov, *Doklady Akad. Nauk USSR* **95**:773, 1177 (1954); **96**:261 (1954); L.D. Landau, I. Pomeranchuk, *Doklady Akad. Nauk USSR* **102**:488 (1955).

[9] R.K. Ellis, in *DPF92 Proceedings*, ed. C.H. Albright, P.H. Kasper, R. Raja, J. Yoh. Singapore: World Scientific (1993).

[10] S. Catani, M. Ciafaloni, F. Hauptmann, *Phys. Lett.* **B242** : 97 (1990); *Nucl. Phys.* **B366** : 135 (1991); R.K. Ellis, D.A. Ross, *Nucl. Phys.* **B45** : 79 (1990); J.C. Collins, R.K. Ellis, *Nucl. Phys.* **B360** : 3 (1991); E.M. Levin, M.G. Ryskin, Yu.M. Shabelsky, A.G. Shuvaev, *Sov. J. Nucl. Phys.* **54** : 867 (1991).

[11] K. Charchula, E.M. Levin, in *Proceedings of the Workshop "Physics at HERA"*, ed. W. Buchmueller, G. Ingelman. Hamburg:DESY, volume 1:223 (1991).

[12] L.V. Gribov, Yu.L Dokshitzer, V.A. Khoze, S.I. Troyan, *Sov. Phys.* JETP **88** : 1303 (1988).

[13] S. Bethke, in *Proceedings of the Workshop "QCD - 20 Years Later"*, ed. P.M. Zerwas, H.A. Kastrup. Volume 1:43 (1992); B.R. Webber In *Proceedings of the Workshop "QCD - 20 Years Later"*, ed. P.M. Zerwas, H.A. Kastrup. Volume 1:73 (1992).

[14] J.E. Huth, M.L. Mangano, Fermilab preprint FERMILAB - PUB-93/19-E. *Ann. Rev. Nucl. Part. Sci.* **43**). In press.

[15] P. Abreu, et al (DELPHI Collaboration). *Phys. Lett.* **B255** : 466 (1991); D. Decamp, et al (ALEPH Collaboration). *Phys. Lett.* **B284** : 151 (1992).

[16] Yu.L. Dokshitzer, V.A. Khoze, A.H. Mueller, S.I. Troyan. *Basics of Perturbative QCD.* Gif-sur-Yvette Cedex: Editions Frontieres (1992).

[17] J.C. Collins, D.E. Soper, G. Sterman. *Nucl. Phys.* **B308** : 833 (1988); J.C. Collins, D.E. Soper, G. Sterman, in *Perturbative Quantum Chromodynamics* , ed. AH Mueller. Singapore: World Scientific (1989) and references therein.

[18] A.S. Kronfeld, P.B. Mackenzie, *Ann. Rev. Nucl. Part. Sci.* **43** : 793 (1993).

[19] M.A. Shifman, in *Proceedings of the Workshop "QCD - 20 Years Later"*, ed. P.M. Zerwas, H.A. Kastrup. Volume 2:775 (1992).

[20] A. DeRoeck (H1 Collaboration), *J. Phys.* **G19**:1549 (1993); S.R. Magill (ZEUS Collaboration), *J. Phys.* **G19**:1535 (1993); M. Besanson (H1 Collaboration), to appear in *Proceedings of Blois Workshop on Elastic and Diffractive Scattering*, Brown University, Providence, June 1993; M. Krzyzanowski (ZEUS Collaboration), to appear in *Proceedings of Blois Workshop on Elastic and Diffractive Scattering*, Brown University, Providence, June 1993.

[21] E.A. Kuraev, L.N. Lipatov, V.S. Fadin, *Sov. Phys. JETP* **45**:199 (1977); Ya.Ya. Balitskii, L.N. Lipatov, *Sov. J. Nucl. Phys.* **28**:822 (1978); L.N. Lipatov, *Sov. Phys. JETP* **63**:904 (1986).

[22] V.N. Gribov, L.N. Lipatov, *Sov. J. Nucl. Phys.* **15**:438 (1972); L.N. Lipatov, *Yad. Fiz.* **20**:181 (1974); G. Altarelli, G. Parisi, *Nucl. Phys.* **B126** : 298 (1977); Yu.L. Dokshitzer, *Sov.Phys. JETP* **46**:641 (1977).

[23] L.V. Gribov, E.M. Levin, M.G. Ryskin, *Phys.Rep.* **100**:1 (1983).

[24] A.H. Mueller, *Nucl. Phys.* **B335** : 115 (1990); *Nucl. Phys.* **B317** : 573 (1989); *Nucl. Phys.* **B307** : 34(1988).

[25] M. Ciafaloni, *Nucl. Phys.* **B296** : 249 (1987); G. Marchesini, B. Webber, *Nucl. Phys.* **B310** 88 :435 (1988); S. Catani, F. Fiorani, G. Marchesini, *Nucl. Phys.* **B336** : 18 (1990); S. Catani, F. Fiorani, G. Marchesini, G. Oriani G, *Nucl. Phys. B (Proc. Suppl.)* **18C**:30 (1990).

[26] G. Marchesini, in *Proceedings of Erice Eloisatron Workshop in Perturbative QCD*, ed. L. Cifarelli, Yu.L. Dokshitzer, Singapore: World Scientific. In press.

[27] F. Abe, et al (CDF Collaboration), *Phys. Rev. Lett.* **68** : 1104 (1992); S. Ellis, Z. Kunszt, D.E. Soper, *Phys. Rev. Lett.* **69** : 3615 (1992).

[28] J.P. Blaizot, A.H. Mueller, *Nucl. Phys.* **B289** : 847 (1987).

[29] L. Landau, I. Pomeranchuk, *Doklady Akad. Nauk USSR* **92**:535 (1953); **92**:735 (1953); A.B. Migdal, *Phys.Rev.* **103**: 1811 (1956); *Sov. Phys.* JETP **5** : 527 (1957).

[30] S T. Stanev, Ch. Vankov, R.E. Streitmatter, R.W. Ellsworth, T. Bowen, *Phys. Rev.* **D25** : 1291 (1982) and references therein.

[31] M. Gyulassy, X-N. Wang, Lawrence Berkeley Laboratory preprint LBL-32682.

[32] S. Klein, et al (SLAC E-146 Collaboration). SLAC preprint SLAC-PUB-6378.

[33] K. Geiger, B. Mueller, *Nucl. Phys.* **B369** : 600 (1911).

[34] K. Geiger, *Phys. Rev.* **D46** : 4986 (1992); *Phys. Rev.* **D47** : 133 (1993); *Phys. Rev. Lett.* **70** : 1290 (1993); *Phys. Rev.* **D48** : 4129 (1993); *Phys. Rev. Lett.* **71** 3 075 (1993); K. Geiger, J.I. Kapusta, *Phys. Rev.* **D47** : 4905 (1993).

[35] A.H. Mueller, J. Qiu, *Nucl. Phys.* **B268**:427 (1986).

[36] E. Levin, M. Wuesthoff, Fermilab preprint FERMILAB-PUB-92/334-T.

[37] J. Bartels, M.G. Ryskin, DESY preprint DESY-93-081.

[38] R.K. Ellis, W. Furmanski, R. Petronzio, *Nucl. Phys.* **B207** : 1 (1982); *Nucl. Phys.* **B212** : 29 (1983).

[39] A. Donnachie, P.V. Landshoff, *Nucl. Phys.* **B244** : 322 (1984); *Nucl. Phys.* **B267** : 690 (1986); P.V. Landshoff, in *Proc. of the LP - HEP'91 Conference.* Volume 2:363, Singapore: World Scientific (1992).

[40] E.M. Levin, M.G. Ryskin, *Phys. Rep.* **189**:267 (1990).

[41] A.D. Martin, *J. Phys.* **G19**:1603 (1993) and references therein.

[42] A.J. Askew, J. Kwiecinski, A.D. Martin, P.J. Sutton PJ, *Phys. Rev.* **D 47**:3775 (1993); J. Kwiecinski, *J. Phys.* **G19**:1443 (1993) and references therein.

[43] V. Braun, M. Gornicki, L. Mankievicz, A. Shafer, *Phys. Lett.* **B302** : 291 (1993).

[44] J.C. Collins, J. Kwiecinski, *Nucl. Phys.* **B335** : 89 (1990).

[45] J. Bartels, J. Blumlein, G. Schuler, *Z. Phys.* **C50** : 91 (1991).

[46] E. Levin, *J. Phys.* **G19**:1453 (1993) and references therein.

[47] H. Abramowicz, E.M. Levin, A. Levy, U. Maor, *Phys. Lett.* **B269** : 465 (1991).

[48] J.C. Collins, G.A. Ladinsky GA, *Phys. Rev.* **D43** : 2847 (1991).

[49] E.L. Feinberg, D.S. Chernavsky, *Usp. Fiz. Nauk* **82**:41 (1964); V.N. Gribov, *Yad. Fiz.* **9** : 640 (1969).

[50] A.H. Mueller, H. Navelet, *Nucl. Phys.* **B 282**:727 (1987).

[51] A.H. Mueller, *Nucl. Phys. B (Proc. Suppl.)* **18C**:125 (1991); J. Bartels, A. De Roeck, M. Loewe, *Z. Phys.* **C54** : 635 (1992); J. Kwiecinski, A.D. Martin, P.J. Sutton, *Phys. Lett.* **B287** : 254 (1992); *Phys. Rev.* **D46** : 921 (1992); W-K. Tang, *Phys. Lett.* **B278** : 363 (1991); J. Bartels, *J. Phys.* **G19**:1611 (1993); E. Laenen, E. Levin, *J. Phys.* **G19**:1582 (1993).

[52] W.J. Stirling, Durham preprint DTP-94-04.

[53] G. Ingelman, P.E. Schlein, *Phys. Lett.* **B152** : 256 (1985); J. Bartels, G. Ingelman, *Phys. Lett.* **B235** : 125 (1990); G. Ingelman, K. Janson-Prytz, *Phys. Lett.* **B281** : 325 (1992).

[54] L.L. Frankfurt, M. Strikman, *Phys. Rev. Lett.* **63** : 1914 (1989); M.G. Ryskin, *Yad. Fiz.* **50** : 1428 (1989); *Sov. J. Nucl. Phys.* **52** : 529 (1990); J.C. Collins, L.L. Frankfurt, M. Strikman, *Phys. Lett.* **B307** : 161 (1993).

[55] N.N. Nikolaev, B.G. Zakharov, *Phys. Lett.* **B260** : 414 (1991); *Z. Phys.* **C49** : 607 (1991); *Z. Phys.* **C53** : 331 (1992), preprint KFA-IKP-1993 -17; V. Barone, M. Genovese, N.N. Nikolaev, E. Predazzi, B.G. Zakharov, *Phys. Lett.* **B268** : 279 (1991); *Phys. Lett.* **B304** : 176 (1993); E. Levin, M. Wuesthoff, Fermilab preprint FERMILAB-PUB-92/334-T; M.G.

Ryskin, M. Besancon, in *Proc. of the Workshop "Physics at HERA"* ed. W. Buchmuller, G. Ingelman. Hamburg:DESY, volume 1:215 (1991).

[56] J.D. Bjorken, *Phys. Rev.* **D45** 4 077 (1992); *Phys. Rev.* **D47** : 101(1992); *Nucl.Phys. B (Proc. Suppl.* **23C**:250 (1992); *Acta Phys. Pol.* **B 23**:637 (1992).

[57] Yu.L. Dokshitzer, V.A. Khoze, T. Sjostrand, *Phys. Lett.* **B274** : 116 (1992).

[58] E. Gotsman, E.M. Levin, U. Maor, *Phys. Lett.* **B309** : 199 (1993).

[59] E. Levin, *Phys. Rev.* **D48** : 2097 (1993).

[60] V. Del Duca, W-K. Tang, *Phys. Lett.* **B312** 2 25 (1993); V. Del Duca, DESY preprint DESY-93-135; SLAC preprint SLAC-PUB-6389.

[61] A.H. Mueller, W-K. Tang, *Phys. Lett.* **B284** : 123 (1992).

[62] S. Feber, "Rapidity Gap Result from D0", *Talk at XXII International Symposium on Multiparticle Dynamics*, Aspen,Colorado, 13 - 17 Sept. 1993.

[63] E.M. Levin, M.G. Ryskin, *Sov. J. Nucl. Phys.* **41** : 300 (1985).

[64] J. Qiu, *Nucl. Phys.* **B291** : 746 (1987); K.J. Eskola, J. Qiu, X-N. Wang, Lawrence Berkeley Laboratory preprint LBL-34156.

[65] J. Gomez, et al, SLAC preprint SLAC-PUB-5813(E).

[66] E. Shuryak, *Phys. Rev. Lett.* **68** : 3278 (1992).

[67] J. Kwiecinski, *Z. Phys.* **C29** : 561 (1985); E.M. Levin, *Orsay Lectures.* Orsay preprint LPTHE-91/02; M. Krawczyk, *Nucl.Phys. B (Proc. Suppl.)* **18C**:64 (1990); V.S. Fadin, L.N. Lipatov, *Nucl. Phys.* **B406** 2 59 (1993).

[68] A.H. Mueller, Columbia preprint CU-TP-609.

[69] A.H. Mueller AH, in *Proceedings of the Workshop "QCD - 20 Years Later"*, ed. P.M. Zerwas, H.A. Kastrup. Volume 1:162 (1992).

[70] Ya. Ya. Balitsky, V.M. Braun, *Nucl. Phys.* **B380** : 51 (1992); *Phys. Lett.* **B314** : 237 (1992); *Phys. Rev.* **D47** : 1879 (1993).

[71] E. Laenen, E. Levin, A.G. Shuvaev, Fermilab preprint FERMILAB-PUB-93/243-T *Nucl.Phys.* **B** in press.

[72] J. Bartels, DESY preprint DESY-93-028; *Phys. Lett.* **B298** : 204 (1993); E.M. Levin, M.G. Ryskin, A.G. Shuvaev, *Nucl.Phys.* **B 387**:589 (1992).

[73] L.N. Lipatov, *Phys. Lett.* **B389** : 394 (1993); *Phys. Lett.* **B365** : 614 (1991).

[74] H. Verlinde, E. Verlinde, Princeton preprint PUPT-1319.

[75] D. Kharzeev, H. Satz; *Z. Phys.* **C60** : 389 (1993); CERN preprint CERN-TH-7115/93.